bioRxiv preprint doi: https://doi.org/10.1101/636514; this version posted May 11, 2020. The copyright holder for this preprint (which was not certified by peer review) is the author/funder, who has granted bioRxiv a license to display the preprint in perpetuity. It is made available under aCC-BY-NC-ND 4.0 International license.

A systems genetics approach reveals environment-dependent associations between SNPs, protein co-expression and drought-related traits in maize

Running title: Systems genetics of drought-related traits in maize

Mélisande Blein-Nicolas[1*], Sandra Sylvia Negro[1], Thierry Balliau[1], Claude Welcker[2], Llorenç Cabrera Bosquet[2], Stéphane Dimitri Nicolas[1], Alain Charcosset[1], Michel Zivy[1*]

[1] Université Paris-Saclay, INRAE, CNRS, AgroParisTech, GQE – Le Moulon, 91190, Gif-sur-Yvette, France

[2] LEPSE, INRAE, Univ Montpellier, SupAgro, Montpellier, France

* Corresponding authors:

michel.zivy@inra.fr, +33-1-69-33-23-65

melisande.blein-nicolas@inra.fr, +33-1-69-15-68-06

Keywords: proteomics, GWAS, drought, Zea mays, mass spectrometry, integrative biology

bioRxiv preprint doi: https://doi.org/10.1101/636514; this version posted May 11, 2020. The copyright holder for this preprint (which was not certified by peer review) is the author/funder, who has granted bioRxiv a license to display the preprint in perpetuity. It is made available under aCC-BY-NC-ND 4.0 International license.

ABSTRACT

The effect of drought on maize yield is of particular concern in the context of climate change and human population growth. However, the complexity of drought-response mechanisms make the design of new drought-tolerant varieties a difficult task that would greatly benefit from a better understanding of the genotype-phenotype relationship. To provide novel insight into this relationship, we applied a systems genetics approach integrating high-throughput phenotypic, proteomic and genomic data acquired from 254 maize hybrids grown under two watering conditions. Using association genetics and protein co-expression analysis, we detected more than 22,000 pQTLs across the two conditions and confidently identified fifteen loci with potential pleiotropic effects on the proteome. We showed that even mild water deficit induced a profound remodeling of the proteome, which affected the structure of the protein co-expression network, and a reprogramming of the genetic control of the abundance of many proteins, notably those involved in stress response. Co-localizations between pQTLs and QTLs for ecophysiological traits, found mostly in the water deficit condition, indicated that this reprogramming may also affect the phenotypic level. Finally, we identified several candidate genes that are potentially responsible for both the co-expression of stress response proteins and the variations of ecophysiological traits under water deficit. Taken together, our findings provide novel insights into the molecular mechanisms of drought tolerance and suggest some pathways for further research and breeding.

bioRxiv preprint doi: https://doi.org/10.1101/636514; this version posted May 11, 2020. The copyright holder for this preprint (which was not certified by peer review) is the author/funder, who has granted bioRxiv a license to display the preprint in perpetuity. It is made available under aCC-BY-NC-ND 4.0 International license.

INTRODUCTION

Maize is the world's leading crop (Shiferaw et al. 2011) in terms of production. Having a C4 metabolism, it exhibits high water use efficiency (WUE). However, it is also highly susceptible to water deficit. For example, maize is more affected by drought than either its close relative sorghum (above-ground dry biomass reduced by 47-51 % and 37-38 %, respectively; Zegada-Lizarazu et al. 2012, Schittenhelm and Schroetter 2014) or wheat, which is a C3 plant (yield reduction associated with a 40% water reduction of 40% and 20.6%, respectively; Daryanto et al. 2016). Improving maize yield under drought has been an important aim of breeding programs for decades (Campos et al. 2004, 2006; Cooper et al. 2014). However, despite the overall genetic improvement of maize, increases in drought sensitivity have been reported in several regions (Lobell et al. 2014; Zipper et al. 2016; Meng et al. 2016). In addition, severe episodes of drought are projected to become more frequent in the near future due to climate change (Harrison et al. 2014). Therefore, maize productivity under water deficit is of particular concern and large efforts are still required to design varieties that are able to maintain high yields in drought conditions.

One lever to accelerate crop improvement is to better understand the genetic and molecular bases of drought tolerance. This highly complex trait is associated with a series of mechanisms occurring at different spatial and temporal scales to (i) stabilize the plant's water and carbon status, (ii) control the side effects of water deficit including oxidative stress, mineral deficiencies and reduced photosynthesis and (iii) maintain plant yield (Chaves et al. 2003). At the physiological level, short-term responses include stomata closure, adjustment of osmotic and hydraulic conductance, leaf growth inhibition and root growth promotion (Tardieu et al. 2018). At the molecular level, complex signaling and regulatory events occur, involving several hormones, of which abscisic acid (ABA) is a key player, and a broad range of transcription factors (Golldack et al. 2014; Osakabe et al. 2014; Tripathi et al. 2014). Molecular responses also include the accumulation of metabolites involved in osmotic adjustment, membrane and protein protection, as

bioRxiv preprint doi: https://doi.org/10.1101/636514; this version posted May 11, 2020. The copyright holder for this preprint (which was not certified by peer review) is the author/funder, who has granted bioRxiv a license to display the preprint in perpetuity. It is made available under aCC-BY-NC-ND 4.0 International license.

well as scavenging of reactive oxygen species, and the expression of drought-responsive proteins such as dehydrins, late embryogenesis abundant (LEA) and heat shock proteins (HSP) (Valliyodan and Nguyen 2006; Seki et al. 2007). All these responses will depend on the drought scenario, the phenological stage, the genetic makeup and the general environmental conditions (Tardieu et al. 2018). Taken together, the multiplicity and versatility of the mechanisms involved explain the difficulty in selecting for drought tolerance.

A better understanding of the genotype-phenotype relationship will help guide the development of new drought-tolerant varieties. Systems genetics is a recent approach providing improved insight into this relationship by deciphering the biological networks and molecular pathways underlying complex traits and by investigating how these traits are regulated at the genetic and epigenetic levels (Nadeau and Dudley 2011; Civelek and Lusis 2014; Feltus 2014; van der Sijde et al. 2014; Markowetz and Boutros 2015). This approach compares the position of quantitative trait loci (QTLs) underlying phenotypic traits variation to that of QTLs underlying the variation of upstream molecular traits such as transcript expression (eQTLs) or protein abundance (pQTLs). Until recently, this approach had been mostly applied in human and mice (Moreno-Moral and Petretto 2016) In plants, systems genetics studies have been carried out in a few species including wheat (Munkvold et al. 2013), rapeseed (Basnet et al. 2016), eucalyptus (Mizrachi et al. 2017) and maize (Christie et al. 2017; Jiang et al. 2019).

The first studies comparing QTLs and pQTLs used 2D gel proteomics to quantify proteins (Bourgeois et al. 2011; de Vienne et al. 1999). Since then, proteome coverage and data reliability have been widely improved by the use of mass spectrometry (MS)-based proteomics (Wasinger et al. 2013). Despite these technical advancements, the systems genetics studies published so far have preferentially used transcripts rather than proteins as the intermediate level between the genome and phenotypic traits. One reason is that large-scale proteomics experiments remain challenging (Blein-Nicolas et al. 2015) due to technical constraints (Balliau et al. 2018) and the trade-off between depth of coverage and sample throughput (Keshishian et al. 2017). However, proteins are

bioRxiv preprint doi: https://doi.org/10.1101/636514; this version posted May 11, 2020. The copyright holder for this preprint (which was not certified by peer review) is the author/funder, who has granted bioRxiv a license to display the preprint in perpetuity. It is made available under aCC-BY-NC-ND 4.0 International license.

particularly relevant molecular components for linking genotype to phenotype. Indeed, proteins abundance is expected to be more highly related to phenotype than transcript expression due to the buffering of transcriptional variations and the role of post-translational regulations in phenotype construction (Foss et al. 2011; Battle et al. 2015; Chick et al. 2016; Albertin et al. 2013; Vogel and Marcotte 2012).

Here, we aimed to better understand the molecular mechanisms associated with the genetic polymorphisms underlying the variations of ecophysiological traits related to drought tolerance. To this end, we performed a novel systems genetics study where MS-based proteomics data acquired from 254 maize genotypes grown in two watering conditions were integrated with high-throughput genomic and phenotypic data. First, protein abundance was analyzed using a genome wide association study (GWAS) and co-expression networks. Then, these data were integrated with ecophysiological phenotypic data from the same experiment (Prado et al. 2018) using a correlation analysis and by searching for QTL/pQTL co-localizations.

bioRxiv preprint doi: https://doi.org/10.1101/636514; this version posted May 11, 2020. The copyright holder for this preprint (which was not certified by peer review) is the author/funder, who has granted bioRxiv a license to display the preprint in perpetuity. It is made available under aCC-BY-NC-ND 4.0 International license.

RESULTS

Mild water deficit has extensively remodeled the proteome

Using MS-based proteomics, we analyzed more than 1,000 leaf samples taken from 254 genotypes representing the genetic diversity within dent maize and grown in well-watered (WW) and water deficit (WD) conditions. After data filtering, the peptide intensity dataset included 977 samples corresponding to 251 genotypes from which we quantified 2,055 proteins described in Supplemental Table S1. Among these, 973 were quantified by integration of peptide intensities (XIC-based quantification). The remaining 1,082, whose peptides had more than 10% of missing intensity values, were quantified by spectral counting (SC-based quantification). Note that the latter proteins were less abundant (Supplemental Fig. S1A) and less precisely quantified (Supplemental Fig. S1B) than those that could be quantified by XIC.

Heatmap representations of protein abundance showed that two large separate protein clusters were associated with the two watering conditions (Fig. 1A). This indicates that, although moderate, water deficit had extensively remodeled the proteome of most genotypes. Accordingly, 82.4% and 74.5% of proteins from the XIC-based and SC-based sets, respectively, responded significantly to water deficit (Supplemental Table S1, Supplemental Figure S2A). These included several proteins known to be involved in responses to drought or stress (Shinozaki & Yamaguchi-Shinozaki 2007; Wang et al. 2016) such as dehydrins (GRMZM2G079440, GRMZM2G373522), an ABA-responsive protein (GRMZM2G106622), an LEA protein (GRMZM2G352415), HSPs (GRMZM2G360681, GRMZM2G080724, GRMZM2G112165), a phospholipase D (GRMZM2G061969), a glyoxalase I (GRMZM2G181192) and a gluthathione-S-transferase (GRMZM2G043291). Induced and repressed proteins constituted two highly differentiated populations in terms of function (Fig. 1B). In particular, transcription, translation, energy metabolism and metabolism of cofactors and vitamins were better represented within repressed

bioRxiv preprint doi: https://doi.org/10.1101/636514; this version posted May 11, 2020. The copyright holder for this preprint (which was not certified by peer review) is the author/funder, who has granted bioRxiv a license to display the preprint in perpetuity. It is made available under aCC-BY-NC-ND 4.0 International license.

proteins, while carbohydrate and amino acid metabolism and environmental adaptation were better represented within induced proteins.

The global impact of genotypic change on the proteome was less extensive than that of water deficit, since the proteomes of two different genotypes grown in the same watering condition were more similar than the proteomes of a same genotype grown in different conditions (Fig. 1A). However, the maximum amplitudes of abundance variations were similar (Supplemental Fig. S2B). In addition, 94.9% of proteins from the XIC-based set exhibited significant variation in abundance attributable to genetic variation (Supplemental Table S1). This was confirmed by broad sense heritability, the median of which was 0.47 and 0.46 for WW and WD conditions, respectively (Supplemental Fig. S3A). By contrast, in the SC-based set, only 34.4% of the proteins showed significant variation in abundance attributable to genetic variation with a median broad sense heritability of 0.08 and 0.10 for WW and WD conditions, respectively (Supplemental Fig. S3B).

Significant GxE interactions were detected for only four and 12 proteins from the SC-based and XIC-based set, respectively, probably due to a lack of statistical power. These proteins included an LEA protein (GRMZM2G352415), a HSP (GRMZM2G083810_P01) and a COR410 dehydrin (GRMZM2G147014_P01). Although the GxE interaction was not statistically significant for the dehydrin ZmRab17 (GRMZM2G079440), this protein was remarkable because it was undetectable in the WW condition and more or less expressed, depending on genotype, in the WD condition (Fig. 1C, Supplemental Table S2).

The strength of the genetic control of protein abundance is related to protein function

We performed GWAS for 2,501 combinations of protein abundance x watering condition showing a heritability > 0.2. In total, we detected 514,270 significant associations for 2,466 (98.6%) combinations of protein abundance x watering condition involving 1,367 proteins. When summarizing associated SNPs into pQTLs using classical methods based on genetic distance or linkage disequilibrium (LD), we observed a positive relationship between the number of pQTLs per

bioRxiv preprint doi: https://doi.org/10.1101/636514; this version posted May 11, 2020. The copyright holder for this preprint (which was not certified by peer review) is the author/funder, who has granted bioRxiv a license to display the preprint in perpetuity. It is made available under aCC-BY-NC-ND 4.0 International license.

chromosome and the *P-value* of the most strongly associated pQTL from the corresponding chromosome (Supplemental Fig. S4A,B). To get rid of this artefactual relationship, which could lead to the detection of more than 250 pQTLs on one chromosome, we developed a geometric method based on the *P-value* signal of SNPs (Supplemental Fig. S4C). This method produced the lowest number of pQTLs per combination of protein abundance x watering condition (median = 8 *vs* 13 for the two other methods) and the lowest maximum number of pQTLs per chromosome (18 *vs* 272 and 209 for the methods based on genetic distance and LD, respectively). Using this geometric method and considering only pQTLs accounting for more than 3% of the total variance, we thus detected 22,664 pQTLs accounting for 3 to 77.1% of the variance (Supplemental Table S3). Of these, 1,113 were local, *i.e.* located less than 10^6 bp from the protein encoding gene, of which 339 were located within the genes. Among distant pQTLs, 80.9% were located on a different chromosome from that of the protein encoding gene. Local pQTLs had stronger effects than distant pQTLs (average *R2*=15.3% and 5.2%, respectively; Supplemental Fig. S5). For 485 proteins, no local pQTL was detected in either condition. This set of proteins was significantly enriched in proteins involved in translation (15.3% *vs* 3.8%, adjusted *P-value* = $2.3E^{-10}$) and energy metabolism (17.3% *vs* 8.5%, adjusted *P-value* = $8.2E^{-5}$) and depleted in proteins involved in carbohydrate metabolism (9.9% *vs* 19.5%, adjusted *P-value* = $8.2E^{-5}$) compared to the 662 proteins showing a local pQTL in at least one condition. They also exhibited fewer distant pQTLs and were much less heritable (Supplemental Fig. S6). These results indicate that the strength of the genetic control over protein abundance depends on protein function. This observation is supported by the positive correlation between the mean number of pQTLs and the mean heritability per functional category (Fig. 2).

Identification of loci with potential pleiotropic effects on the proteome

pQTLs were not uniformly distributed in the genome (Fig. 3). Instead, there were genomic regions enriched with pQTLs. We detected 26 and 31 such hotspots that contained at least 19

bioRxiv preprint doi: https://doi.org/10.1101/636514; this version posted May 11, 2020. The copyright holder for this preprint (which was not certified by peer review) is the author/funder, who has granted bioRxiv a license to display the preprint in perpetuity. It is made available under aCC-BY-NC-ND 4.0 International license.

pQTLs in the WW and WD conditions, respectively (Supplemental Table S4). These hotspots may represent loci with pleiotropic effects on the proteome, *i.e.* loci associated with the abundance variation of several proteins. To refine the detection of such loci, we used a second independent approach based on the search for co-expression QTLs (coQTLs), *i.e.*, QTLs associated to the abundance variations of several co-expressed proteins. To do so, we first performed a weighted gene co-expression network analysis (WGCNA) of protein co-expression across the 251 genotypes in the two watering conditions separately (Supplemental Table S5). The two resulting networks differed in the presence of condition-specific modules indicating that water deficit has altered the structure of the protein co-expression network (Fig. 4, Supplemental Fig. S7, Supplemental File S1). For each co-expression module, we then submitted the representative variable, called eigengene according to the WGCNA terminology, to GWAS in order to identify coQTLs. In total, we detected 176 coQTLs (96 for the 8 WW modules and 80 for the 8 WD modules, Supplemental Table S3). Fifteen of them co-localized with pQTL hotspots (Supplemental Table S4). Thus by crossing these results, we confidently identified four loci in the WW condition and eleven loci in the WD condition as having potential pleiotropic effects on the proteome. Of note, the proteins that were associated with hotspots Hs22d and Hs21d and that were also in the modules having coQTLs co-localising with these hotspots were mainly ribosomal proteins (Supplemental Table S6). This suggests that Hs22d and Hs21d may contain loci involved in ribosome biogenesis.

The genetic architecture of protein abundances depends on the environment

Of the 11,034 pQTLs detected in the WW condition, only 1,124 (10.2%) had a co-localizing pQTL in the WD condition. These pQTLs were generally of strong effect (Supplemental Fig. S8A) and were enriched in local pQTLs (32.6% *vs* 4.9% over the entire dataset). While most of the pQTLs that were common to the two conditions had similar effects in both conditions, 75 (6.7%) of them exhibited contrasted effects (Supplemental Fig. S8B). Half of these pQTLs were local, suggesting that gene promoters may be involved in the GxE interaction or that the pQTLs that were

bioRxiv preprint doi: https://doi.org/10.1101/636514; this version posted May 11, 2020. The copyright holder for this preprint (which was not certified by peer review) is the author/funder, who has granted bioRxiv a license to display the preprint in perpetuity. It is made available under aCC-BY-NC-ND 4.0 International license.

detected in each condition corresponded to different polymorphic sequences with different effects on protein abundance. These pQTLs were associated with 70 proteins, several of which were stress-responsive (*e.g.* the LEA protein GRMZM2G045664, HSPs GRMZM5G813217 and GRMZM2G536644, Supplemental Table S7). Altogether, these results show that water deficit has altered the genetic architecture of protein abundance.

Identification of loci associated with trait variation at multiple scales

To gain insight into the molecular mechanisms associated with drought tolerance, we searched for co-localizations between the pQTLs, coQTLs and hotspots detected in our study and the 160 QTLs identified by Prado et al. (2018) on the same plant material. These QTLs were associated with eight ecophysiological traits related to growth and transpiration rate: early leaf area (*i.e.* before water deficit; LAe), late leaf area (LAl), early biomass (Be), late biomass (Bl), water use (WU), water use efficiency (WUE), stomatal conductance (gs) and transpiration rate (Trate). Robust co-localizations were determined by taking into account the correlation between each trait and protein values.

In total, we identified 68 pairs of SNPs corresponding to QTL/pQTL co-localizations (Fig. 5, Supplemental Table S8). Only one involved a local pQTL. The QTL/pQTL distance was generally less than 100 kb, with, in 25.7% of cases, the same SNP representing the QTL and the pQTL (Fig. 6A). Most QTL/pQTL co-localizations (98%) were detected in the WD condition, where they corresponded to 39 of the 91 QTLs reported in this condition (Prado et al. 2018). They involved six ecophysiological phenotypic traits (Bl, LAl, WU, WUE, Trate and gs) and 47 proteins, many of which were stress-responsive (Supplemental Table S9). Twenty-three proteins exhibited multiple QTL/pQTL co-localizations (Supplemental Table S9).

We further identified 11 pairs of SNPs corresponding to QTL/coQTL co-localizations, all in the WD condition (Supplemental Table S10). They involved three phenotypic traits (WU, Bl, LAl) and two co-expression modules including the WD-specific module (Fig. 5). These two modules

bioRxiv preprint doi: https://doi.org/10.1101/636514; this version posted May 11, 2020. The copyright holder for this preprint (which was not certified by peer review) is the author/funder, who has granted bioRxiv a license to display the preprint in perpetuity. It is made available under aCC-BY-NC-ND 4.0 International license.

were significantly enriched in stress-response proteins and in proteins involved in hormone metabolim and in reactive oxygen species detoxification (Supplemental Table S11). Ten of the 11 QTLs co-localizing with coQTLs also co-localized with pQTLs. The remaining QTL actually also co-localized with pQTLs, but with a low correlation between the phenotypic trait values and the protein abundance levels ($|r_{corrected}| < 0.23$; Supplemental Table S10). By contrast, the correlation between trait values and eigengene was much higher ($|r_{corrected}| = 0.51$), which indicates that proteins were more strongly related to ecophysiological traits when taken collectively through a co-expression module rather than taken individually.

Taken together, these results highlight the presence of loci associated with traits at different biological scales. In the WD condition, several of these loci showed multiple associations both at the proteome and the phenotype level (Fig. 5). On Chromosome 1, a locus spanning 33 kbp contained a QTL for LAl determined by SNP S1_5382845 as well as a coQTL for the green module and seven pQTLs, all determined by SNP AX-91427638. On Chromosome 5, a locus spanning 1.8 Mb between SNPs AX-91657926 and AX-91658235, contained three QTLs for LAl, Bl and WU, one coQTLs for the WD-specific module and six pQTLs. This region also contained hotspot Hs52d. On Chromosome 7, a single SNP (S7_162671160) determined the positions of two QTLs for LAl and WU, two coQTLs and seven pQTLs. On Chromosome 10, a locus spanning 1.3 Mb between SNPs S10_122802154 and S10_124095144, contained one QTL for LAl, one coQTL and eight pQTLs. This region also contained hotspot Hs103d. Note that in the WD condition, leaf area (LAl) was repeatedly associated with the green module (on Chromosomes 1, 7, 9, 10) and to proteins belonging to this module. Several of them were detoxification enzymes (*i.e.*, a putative polyphenol oxydase, GRMZM5G851266; two peroxydases, GRMZM2G085967 and GRMZM2G108153; a superoxide dismutase GRMZM2G025992; a glyoxalase GRMZM2G704005).

Identification of candidate genes potentially involved in drought tolerance

bioRxiv preprint doi: https://doi.org/10.1101/636514; this version posted May 11, 2020. The copyright holder for this preprint (which was not certified by peer review) is the author/funder, who has granted bioRxiv a license to display the preprint in perpetuity. It is made available under aCC-BY-NC-ND 4.0 International license.

Assuming that the genetic polymorphisms associated with protein abundance variations are within genes, we retrieved a list of one to 49 candidate genes for each of the 69 pairs of SNPs corresponding to a QTL/pQTL or QTL/coQTL co-localization (Supplemental Table S12). Based on gene annotation and the literature, we identified two particularly interesting cases.

First, on Chromosome 7, the SNP S7_162671160 was located in *ZmGH3.8* (GRMZM2G053338), which was the only candidate gene. *ZmGH3.8* is involved in indole-3-acetyl-amide conjugate biosynthesis. In agreement with the role of this gene in drought response (Feng et al. 2015), S7_162671160 was associated with the WD-specific module, WU and LAl and five stress-response proteins (endochitinase GRMZM2G051943, beta-D-glucanase GRMZM2G073079, peroxidase GRMZM2G085967, polyphenol oxydase GRMZM5G851266 and phospholipase D GRMZM2G061969).

Second, 14 candidate genes were identified in the region of Chromosome 5 covered by hotspot Hs52d, of which two could be associated with the expression variation of a high number of genes. One is a squamosa promoter-binding (SBP) gene (GRMZM2G111136) that is inducible by various abiotic stresses including drought (Mao et al. 2016). The other, a C2C2-CO-like transcription factor (GRMZM2G148772), was found to be significantly induced by drought and salinity stress in B73 leaves (Forestan et al. 2016). Hotspot Hs52d covered a region of *ca* 4 Mb in which we detected 26 pQTLs (many of which were located between the SBP gene and the C2C2-CO-like transcription factor), two coQTLs and four QTLs (Fig. 6B). A single SNP, AX-91658235 located only one kbp from the C2C2-CO-like transcription factor, determined the position of two QTLs, two pQTLs and one coQTL. Furthermore, SNP S5_88793314, located within the coding sequence of the SBP gene, determined the position of a QTL and a pQTL. Based on these results, we can hypothesize that hotspot Hs52d may correspond to two trans-acting factors for which the SBP gene and the C2C2-CO-like transcription factor represent good candidates.

bioRxiv preprint doi: https://doi.org/10.1101/636514; this version posted May 11, 2020. The copyright holder for this preprint (which was not certified by peer review) is the author/funder, who has granted bioRxiv a license to display the preprint in perpetuity. It is made available under aCC-BY-NC-ND 4.0 International license.

DISCUSSION

To better understand the molecular mechanisms associated with the genetic polymorphisms underlying the variations in ecophysiological traits related to drought tolerance, we used a proteomics-based systems genetics approach which allowed us to map 22,664 pQTLs at high-resolution. By relating pQTLs to protein functions and heritability, we showed that the level of genetic control over protein abundances depends on protein function. Notably, proteins involved in translation and energy metabolism exhibited few pQTLs, with a lack of local pQTLs and low heritability. As these two functional categories mainly contain ancient and evolutionarily conserved proteins (Goldman et al. 2010; Nelson and Junge 2015), our results suggest that evolutionarily ancient proteins have more constrained expressions and fewer associated pQTLs (Mähler et al. 2017; Popadin et al. 2014; Zhang and Yang 2015). They also support the recent hypothesis of Mähler et al. (2017) that, for genes experiencing reduced rates of molecular evolution, purifying selection on individual SNPs is associated with stabilizing selection on gene expression.

pQTLs were found throughout the genome but some of them clustered into hotspots, suggesting the presence of loci with pleiotropic effects on the proteome. The detection of QTL hotspots is highly dependent on the number of traits studied, the mapping resolution and the method used to cluster QTLs. This may explain why previous studies have reported hotspots ranging from hundreds of eQTLs (Munkvold et al. 2013; Christie et al. 2017; Orozco et al. 2012) to only a few tens of eQTL or pQTLs (Foss et al. 2011; Ghazalpour et al. 2011; Albert et al. 2014) or even no hotspot at all (Mähler et al. 2017). In our study, false hotspot detection was limited by having a high mapping resolution and by using a pQTL clustering method that takes into account LD variations across the genome (Negro et al. 2019). Based on co-localization with coQTLs, we ultimately cross-validated 15 condition-specific hotspots, suggesting that loci with pleiotropic effects on the proteome can interact with the environment.

bioRxiv preprint doi: https://doi.org/10.1101/636514; this version posted May 11, 2020. The copyright holder for this preprint (which was not certified by peer review) is the author/funder, who has granted bioRxiv a license to display the preprint in perpetuity. It is made available under aCC-BY-NC-ND 4.0 International license.

By analyzing a diversity panel of 254 genotypes, we showed that many small changes in protein abundance, detected as significant because they occurred in a high number of genotypes, contributed to extensively remodel the proteome in water deficit conditions. In total, approximately 75% of quantified proteins responded significantly to environmental change. Up- and down regulated proteins were well differentiated in terms of function, and indicated that the photosynthetic, transcriptional and translational machineries were slowed down while stress responses and signalization mechanisms were activated. All these changes showed that plants clearly perceived a lack of water and presented a coordinated proteome response to water deficit.

Changes in abundance occurring in response to water deficit were associated with changes in the structure of the co-expression network. Indeed, we identified condition-specific modules, one of which, in the WD condition, was significantly enriched for stress-response proteins. Similarly, Munkvold et al. (2013) observed condition-specific modules related to biological processes in response to particular environmental conditions. Such modules suggest that, under environmental perturbation, sets of genes or proteins are collectively mobilized by condition-specific factors allowing plant cells to adapt. The WD-specific module was associated with several QTL/coQTL colocalizations and its eigengene was highly correlated with biomass, water use and leaf area. Although the approach used here is correlative, these results suggest that, under water deficit, stress-response proteins contribute to phenotypic responses, which is consistent with the fact that many QTL/pQTL co-localizations involved these types of proteins. One coQTL for the WD-specific module was located in a region of Chromosome 5 that also cumulated several QTLs, pQTLs and the hotspot Hs52d. This indicates that the co-expression observed for stress response proteins may be driven by condition-specific factors, the pleiotropic effects of which resonate across all layers of biological complexity up to phenotype. Altogether, these results suggest that an eigengene may be considered a more integrated molecular trait than protein abundance, and can help decipher the genotype-phenotype relationship by bridging the gap between the proteomic and phenotypic level.

bioRxiv preprint doi: https://doi.org/10.1101/636514; this version posted May 11, 2020. The copyright holder for this preprint (which was not certified by peer review) is the author/funder, who has granted bioRxiv a license to display the preprint in perpetuity. It is made available under aCC-BY-NC-ND 4.0 International license.

Linking phenotypic variation to proteome variation revealed many QTL/pQTL co-localizations for which, using high mapping resolution, we identified a limited number of candidate genes.

Only two of the 69 QTLs detected in the WW condition, *vs* 39 of the 91 in the WD condition, co-localized with pQTLs. This difference could be explained by the hypothesis that under non-stress conditions, phenotypic variations are driven by many low contribution proteins, whose abundance is probably controlled by low effect genetic polymorphisms, whereas under water stress, phenotypic variations are mainly driven by stress response proteins under the genetic control of condition-specific factors. In agreement with this hypothesis, we robustly identified two genomic regions that could correspond to such factors. The first is located on Chromosome 7, where we identified *ZmGH3.8* as the sole candidate gene underlying two QTLs (for leaf area and water use), seven pQTLs, of which five were associated with proteins involved in stress responses, and two coQTLs, one of which was associated with the WD-specific module. In maize shoots, Feng et al. (2015) showed that the expression of *ZmGH3.8* was induced by auxin and reduced under polyethylene glycol treatment. The second region is located on Chromosome 5, in the region of the Hs52d hotspot, where we identified an SBP gene (GRMZM2G111136) and a C2C2-CO-like gene (GRMZM2G148772) as candidate genes underlying four QTLs, six pQTLs and one coQTLs. These two transcription factors have been previously shown to be induced by drought in maize (Mao et al. 2016; Forestan et al. 2016). In addition, SBP genes constitute a functionally diverse family of transcription factors involved in plant growth and development (Preston and Hileman 2013). Due to their potential implication in GxE interactions and because of their roles both in plant growth and development and in drought response, Z*mWRKY48*, *ZmGH3.8*, SBP and C2C2-CO-like genes represent promising candidates for drought tolerance breeding.

To conclude, our systems genetics approach which incorporates MS-based proteomics data has yielded several new results regarding the drought response in maize. First, we point out that the strength of the genetic control over protein abundance is related to protein function and also

bioRxiv preprint doi: https://doi.org/10.1101/636514; this version posted May 11, 2020. The copyright holder for this preprint (which was not certified by peer review) is the author/funder, who has granted bioRxiv a license to display the preprint in perpetuity. It is made available under aCC-BY-NC-ND 4.0 International license.

360 probably to the evolutionary constraints on protein expression. Then, we show that even mild water deficit strongly remodels the proteome and induces a reprogramming of the genetic control of the
362 abundance of many proteins and notably those involved in stress responses. QTL/pQTL co-localizations are mostly found in the WD condition indicating that this reprogramming also affects
364 the phenotypic level. Finally, we identify candidate genes that are potentially responsible for both the co-expression of stress-response proteins and the variation of ecophysiological traits under
366 water deficit. Taken together, our findings provide novel insights into the molecular mechanisms of drought tolerance and suggest some pathways for further research and breeding. Our study also
368 demonstrates that proteomics has now reached enough maturity to be fully exploited in systems studies necessitating large-scale experiments.

bioRxiv preprint doi: https://doi.org/10.1101/636514; this version posted May 11, 2020. The copyright holder for this preprint (which was not certified by peer review) is the author/funder, who has granted bioRxiv a license to display the preprint in perpetuity. It is made available under aCC-BY-NC-ND 4.0 International license.

370 **METHODS**

372 **Plant material and experiment**

Plant material and growth conditions are described in full details in Prado et al. (2018) and in
374 the Supplemental Methods. In brief, a diversity panel of maize hybrids was obtained by crossing a common flint parent (UH007, paternal parent) with 254 dent lines. Two levels of soil water content
376 were applied: well-watered (soil water potential of -0.05 MPa) and water deficit (soil water potential of -0.45 MPa). Hybrids were replicated three times in each watering condition. Leaf
378 sampling was performed at the pre-flowering stage in two replicates per hybrid and water condition.

380 **Protein extraction and digestion**

Protein extraction and digestion procedures are described in full detail in the Supplemental
382 Methods. In brief, proteins were extracted from frozen ground leaf samples using a standard protocol for protein precipitation with trichloroacetic acid and acetone solution. Tryptic digestion
384 was performed after solubilization, reduction and alkylation of the proteins. The resulting peptides were desalted by solid phase extraction using polymeric C18 columns.

386

LC-MS/MS analyses

388 Samples were analyzed by LC-MS/MS in batches of 96. Analyses were performed using a NanoLC-Ultra System (nano2DUltra, Eksigent, Les Ulis, France) connected to a Q-Exactive mass
390 spectrometer (Thermo Electron, Waltham, MA, USA). A 400 ng protein digest was loaded at 7.5 µl.min^{-1} on a Biosphere C18 pre-column (0.3 × 5 mm, 100 Å, 5 µm; Nanoseparation,
392 Nieuwkoop, Netherlands) and desalted with 0.1% formic acid and 2% ACN. After 3 min, the pre-column was connected to a Biosphere C18 nanocolumn (0.075 × 150 mm, 100 Å, 3 µm,
394 Nanoseparation). Buffers were 0.1% formic acid in water (A) and 0.1% formic acid and 100% ACN (B). Peptides were separated using a linear gradient from 5 to 35% buffer B for 40 min at 300

bioRxiv preprint doi: https://doi.org/10.1101/636514; this version posted May 11, 2020. The copyright holder for this preprint (which was not certified by peer review) is the author/funder, who has granted bioRxiv a license to display the preprint in perpetuity. It is made available under aCC-BY-NC-ND 4.0 International license.

396 nl.min^{-1}. One run took 60 min, including the regeneration step at 95% buffer B and the equilibration step at 95% buffer A. Ionization was performed with a 1.4-kV spray voltage applied to an uncoated
398 capillary probe (10 µm tip inner diameter; New Objective, Woburn, MA, USA). Peptide ions were analyzed using Xcalibur 2.2 (Thermo Electron) in a data-dependent acquisition mode as described
400 in the Supplemental Methods.

402 **Peptide and protein identification**

Peptide identification was performed using the MaizeSequence genome database (Release 5a,
404 136,770 entries, https://ftp.maizegdb.org/MaizeGDB/FTP/) supplemented with 1,821 French maize inbred line F2 sequences with present/absent variants (PAVs) (Darracq et al. 2018) and a custom
406 database containing standard contaminants. Database searches were performed using X!Tandem (Craig and Beavis 2004) (version 2015.04.01.1) and protein inference was performed using a
408 homemade C++ version of X!TandemPipeline (Langella et al. 2017) specifically designed to handle hundreds of MS run files. Parameters for peptide identification and protein inference are described
410 in the Supplemental Methods. The false discovery rate (FDR) was estimated at 0.06% for peptides and 0.04% for proteins.

412 Functional annotation of proteins was based on MapMan mapping (Thimm et al. 2004; Usadel et al. 2009) (Zm_B73_5b_FGS_cds_2012 available at https://mapman.gabipd.org/) and on a custom
414 KEGG classification built by manually attributing the MapMan bins to KEGG pathways (Dillmann, pers. com.).

416

Peptide and protein quantification

418 Peptide quantification was performed using MassChroQ version 2.1.0 (Valot et al. 2011) based on extracted ion chromatograms (XIC) with the parameters described in the Supplemental Methods.
420 Peptide quantification data were filtered to remove genotypes represented by only one or two samples instead of the expected four, as well as outlier samples for which we suspected technical

bioRxiv preprint doi: https://doi.org/10.1101/636514; this version posted May 11, 2020. The copyright holder for this preprint (which was not certified by peer review) is the author/funder, who has granted bioRxiv a license to display the preprint in perpetuity. It is made available under aCC-BY-NC-ND 4.0 International license.

problems during sample preparation or MS analysis. In the end, the MS dataset included 977 samples.

Proteins were quantified from peptides using two complementary methods. *i. XIC-based quantification:* Proteins were quantified based on peptide intensity data filtered and normalized as described in the Supplemental Methods. We excluded proteins that were quantified by only one peptide. As samples were analyzed by LC-MS/MS in batches over a period of several months, we observed a strong batch effect on normalized peptide intensities. To correct this batch effect, we fitted a linear model to log-transformed intensity data and subtracted the component due to batch effects. Then, for each protein, we modeled the peptide data using a mixed-effects model derived from Blein-Nicolas et al. (2012) and described in the Supplemental Methods. Protein abundance was subsequently computed as adjusted means from the model's estimates. *ii. Spectral counting (SC)-based quantification:* Proteins that could not be quantified with XIC because their peptides had too many missing intensity values were quantified based on their number of assigned spectra. Proteins with a spectral count < 2 in any of the samples were discarded. Normalization was then performed as described in the Supplemental Methods. As in XIC-based quantification, we corrected the batch effect by fitting a linear model to square-root transformed and normalized protein abundances. Analysis of variance (ANOVA) was subsequently performed using the mixed-effects model described in the Supplemental Methods.

Genome wide association study

GWAS was performed on protein abundances estimated in each watering condition using the single locus mixed model described in Yu et al. (2006). The variance-covariance matrix was determined as described in Rincent et al. (2014) by a kinship matrix derived from all SNPs except those on the Chromosome containing the SNP being tested. SNP effects were estimated by generalized least squares and their significance was tested with an F-statistic. An SNP was

bioRxiv preprint doi: https://doi.org/10.1101/636514; this version posted May 11, 2020. The copyright holder for this preprint (which was not certified by peer review) is the author/funder, who has granted bioRxiv a license to display the preprint in perpetuity. It is made available under aCC-BY-NC-ND 4.0 International license.

considered significantly associated when -$\log_{10}$(*P-value*) > 5. A set of 961,971 SNPs obtained from line genotyping using a 50 K Infinium HD Illumina array (Ganal et al. 2011), a 600 K Axiom Affymetrix array (Unterseer et al. 2014) and a set of 500 K SNPs obtained by genotyping-by-sequencing (Negro et al. 2019) were tested. Analyses were performed with FaST-LMM (Lippert et al. 2011) v2.07. Only SNPs with minor allele frequencies > 5% were considered.

Inflation factors were computed as the slopes of the linear regressions on the QQplots between observed -$\log_{10}$(*P-value*) and expected -$\log_{10}$(*P-value*). Inflation factors were close to 1 (median of 1.08 and 1.06 in the XIC-based and SC-based sets, respectively), indicating low inflation of *P-values*.

Detection of QTLs from significantly associated SNPs

Three different methods implemented in R (R core team 2013) version 3.3.3 were used to summarize significantly associated SNPs into pQTLs. *i. The genetic method:* two contiguous SNPs were considered to belong to a same QTL when the genetic distance separating them was less than 0.1 cM. *ii. The LD-based method:* two contiguous SNPs were considered to belong to a same QTL when their LD-based windows (Negro et al. 2019) overlapped. *iii. The geometric method:* for each chromosome, we ordered the SNPs according to their physical position. Then, we smoothed the -$\log_{10}$(*P-value*) signal by computing the maximum of the -$\log_{10}$(*P-values*) in a sliding window containing *N* consecutive SNPs. An association peak was detected when the smoothed -$\log_{10}$(*P-value*) signal exceeded a max threshold *M*. Two consecutive peaks were considered to be two different QTLs when the -$\log_{10}$(*P-value*) signal separating them dropped below a min threshold *m*. The parameters for QTL detection were fixed empirically at N=500, M=5 and m=4. For the three methods described above, the position of a QTL was determined by the SNP exhibiting the highest -$\log_{10}$(*P-value*). A pQTL was considered local if it was within 1 Mb upstream or downstream of the coding sequence of the gene encoding the corresponding protein.

bioRxiv preprint doi: https://doi.org/10.1101/636514; this version posted May 11, 2020. The copyright holder for this preprint (which was not certified by peer review) is the author/funder, who has granted bioRxiv a license to display the preprint in perpetuity. It is made available under aCC-BY-NC-ND 4.0 International license.

Complementary data analyses

The following complementary data analyses were performed with R (R core team 2013) version 3.3.3. *i. Broad sense heritability of protein abundance:* For each protein, the broad sense heritability of abundance was computed for each of the two watering conditions from a mixed-effects model as described in the Supplemental Methods. *ii. detection of pQTL hotspots:* for each SNP position, we counted the number of pQTLs (*N*) located within its LD-based window (Negro et al. 2019). The threshold used to detect a hotspot was set at the 97% quantile of the distribution of *N*. *iii. Protein co-expression analysis:* Protein co-expression analysis was performed using the WGCNA R package (Langfelder and Horvath 2008) with the parameters described in the Supplemental Methods. Using a procedure developed to correct the bias due to population structure and/or relatedness in the LD measure and implemented in the LDcorSV R package (Mangin et al. 2012), we computed pair-wise Pearson's correlations corrected by structure and kinship ($|r_{corrected}|$) and used them as the input similarity matrix. Graphical representations of the resulting networks were performed with Cytoscape (Shannon et al. 2003) v3.5.1 using an unweighted spring embedded layout. *iv. QTL co-localization:* We considered QTLs to co-localize when they meet the following two criteria. First, the LD-based windows around the QTLs (Negro et al. 2019) should overlap. Second, the absolute value of the Pearson's correlation of coefficient corrected by structure and kinship (the $|r_{corrected}|$ mentioned above) between the values of the ecophysiological traits associated with the QTLs should be greater than 0.3. We determined this value empirically, in the absence of a statistical test to test the significance of the corrected correlation. *v. Candidate gene identification:* For each QTL/pQTL co-localization, gene accessions found within the interval defined by the intersection between the LD-based windows around the QTL and the pQTL were retrieved from the MaizeSequence genome database (Release 5a). Low confidence gene models and transposable elements were not considered.

bioRxiv preprint doi: https://doi.org/10.1101/636514; this version posted May 11, 2020. The copyright holder for this preprint (which was not certified by peer review) is the author/funder, who has granted bioRxiv a license to display the preprint in perpetuity. It is made available under aCC-BY-NC-ND 4.0 International license.

DATA ACCESS

The raw MS output files were deposited online using PROTICdb (Langella et al. 2007; Ferry-Dumazet et al. 2005; Langella et al. 2013) at the following URL: http://moulon.inra.fr/protic/amaizing (DOI 10.15454/1.5736519296148652E12, currently available with the following username: reviewer and password: reviewer) and at MassIVE at the following URL: ftp://MSV000084619@massive.ucsd.edu (doi:10.25345/C5Q684). They will be made freely available after publication. Detailed information on all peptides and proteins identified in the LC-MS/MS runs as well as peptide intensities and protein abundances obtained for each sample are also freely available on PROTICdb at the same URL.

Phenotypic data are available online using the PHIS information system (Neveu et al. 2019) at the following URL: http://www.phis.inra.fr/openphis/web/index.php?r=project%2Fview&id=Systems+genetics+for+maize+drought+tolerance+%28Amaizing+project%29. Earlyeaf area (LAe) was defined at the seven leaves stage, representing 24 $d_{20°C}$ (thermal time in equivalent days at 20°C). Late leaf area (LAl) was defined at the 12 leaves stage, representing 45 $d_{20°C}$.

Genotyping data are available at the following URL: https://doi.org/10.15454/GAHEU0

bioRxiv preprint doi: https://doi.org/10.1101/636514; this version posted May 11, 2020. The copyright holder for this preprint (which was not certified by peer review) is the author/funder, who has granted bioRxiv a license to display the preprint in perpetuity. It is made available under aCC-BY-NC-ND 4.0 International license.

ACKNOWLEDGMENTS

This work was supported by the Agence Nationale de la Recherche project ANT-10-BTBR-01 (Amaizing). Proteomics analyses were performed on the PAPPSO platform (http://pappso.inra.fr) which is supported by INRA (http://www.inra.fr), the Ile-de-France regional council (https://www.iledefrance.fr/education-recherche), IBiSA (https://www.ibisa.net) and Saclay Plant Sciences-SPS (ANR-17-EUR-0007). The authors want to thank Sylvie Coursol for her critical review of the manuscript, Hélène Corti for her help in sample preparation and Olivier Langella for having specially developed a pipeline to upload the proteomics data on ProticDB. They are also grateful to people from INRA LEPSE: François Tardieu for his contribution to the coordination of the plant experiment; Benoît Suard, Pauline Sidawi and Olivier Martin for their technical assistance during the experiment; Santiago Alvarez Prado for his contribution to plant traits and QTL analysis.

AUTHORS CONTRIBUTION

AC and MZ designed the research; CW designed and coordinated the plant experiment in PhenoArch and the genetic analysis of plant traits; LBC performed the plant experiment and analyzed the image-based phenotypic data; MBN and TB performed the proteomics experiments; SSN developed the GWAS pipeline and performed the genotyping quality control; SDN performed the genotyping and estimated local LD; MBN and MZ analyzed the proteomics data, MBN performed the systems genetics study and wrote the manuscript. All authors discussed the results and read and approved the final manuscript.

DISCLOSURE DECLARATION

The authors declare no competing interest.

bioRxiv preprint doi: https://doi.org/10.1101/636514; this version posted May 11, 2020. The copyright holder for this preprint (which was not certified by peer review) is the author/funder, who has granted bioRxiv a license to display the preprint in perpetuity. It is made available under aCC-BY-NC-ND 4.0 International license.

538 **REFERENCES**

Albert FW, Treusch S, Shockley AH, Bloom JS, Kruglyak L. 2014. Genetics of single-cell protein abundance variation in large yeast populations. *Nature* **506**: 494–497.

Albertin W, Marullo P, Bely M, Aigle M, Bourgais A, Langella O, Balliau T, Chevret D, Valot B, da Silva T, et al. 2013. Linking post-translational modifications and variation of phenotypic traits. *Mol Cell Proteomics* **12**: 720–735.

Balliau T, Blein-Nicolas M, Zivy M. 2018. Evaluation of optimized tube-gel methods of sample preparation for large-scale plant proteomics. *Proteomes* **6**.

Basnet RK, Del Carpio DP, Xiao D, Bucher J, Jin M, Boyle K, Fobert P, Visser RGF, Maliepaard C, Bonnema G. 2016. A systems genetics approach identifies gene regulatory networks associated with fatty acid composition in *Brassica rapa* seed. *Plant Physiol* **170**: 568–585.

Battle A, Khan Z, Wang SH, Mitrano A, Ford MJ, Pritchard JK, Gilad Y. 2015. Impact of regulatory variation from RNA to protein. *Science* **347**: 664–667.

Blein-Nicolas M, Albertin W, da Silva T, Valot B, Balliau T, Masneuf-Pomarède I, Bely M, Marullo P, Sicard D, Dillmann C, et al. 2015. A systems approach to elucidate heterosis of protein abundances in yeast. *Mol Cell Proteomics* **14**: 2056–2071.

Blein-Nicolas M, Xu H, de Vienne D, Giraud C, Huet S, Zivy M. 2012. Including shared peptides for estimating protein abundances: A significant improvement for quantitative proteomics. *Proteomics* **12**: 2797–2801.

Bourgeois M, Jacquin F, Cassecuelle F, Savois V, Belghazi M, Aubert G, Quillien L, Huart M, Marget P, Burstin J. 2011. A PQL (protein quantity loci) analysis of mature pea seed proteins identifies loci determining seed protein composition. *Proteomics* **11**: 1581–1594.

Campos H, Cooper M, Edmeades GO, Löffler CM, Schussler JR, Ibáñez M. 2006. Changes in drought tolerance in maize associated with fifty years of breeding for yield in the US Corn Belt. *Maydica* **51**: 369–381.

Campos H, Cooper M, Habben JE, Edmeades GO, Schussler JR. 2004. Improving drought tolerance in maize: a view from industry *Field Crops Res* **90**: 19–34.

Chaves MM, Maroco JP, Pereira JS. 2003. Understanding plant responses to drought — from genes to the whole plant. *Funct Plant Biol* **30**: 239–264.

Chick JM, Munger SC, Simecek P, Huttlin EL, Choi K, Gatti DM, Raghupathy N, Svenson KL, Churchill GA, Gygi SP. 2016. Defining the consequences of genetic variation on a proteome-wide scale. *Nature* **534**: 500–505.

Christie N, Myburg AA, Joubert F, Murray SL, Carstens M, Lin Y-C, Meyer J, Crampton BG, Christensen SA, Ntuli JF, et al. 2017. Systems genetics reveals a transcriptional network associated with susceptibility in the maize–grey leaf spot pathosystem. *Plant J* **89**: 746–763.

Civelek M, Lusis AJ. 2014. Systems genetics approaches to understand complex traits. *Nat Rev Genet* **15**: 34–48.

Cooper M, Gho C, Leafgren R, Tang T, Messina C. 2014. Breeding drought-tolerant maize hybrids for the US corn-belt: discovery to product. *J Exp Bot* **65**: 6191–6204.

Craig R, Beavis RC. 2004. TANDEM: matching proteins with tandem mass spectra. *Bioinformatics* **20**: 1466–1467.

Darracq A, Vitte C, Nicolas S, Duarte J, Pichon J-P, Mary-Huard T, Chevalier C, Bérard A, Le Paslier M-C, Rogowsky P, et al. 2018. Sequence analysis of European maize inbred line F2 provides new insights into molecular and chromosomal characteristics of presence/absence variants. *BMC Genomics* **19**.

Daryanto S, Wang L, Jacinthe P-A. 2016. Global synthesis of drought effects on maize and wheat production. *PLoS ONE* **11**.

bioRxiv preprint doi: https://doi.org/10.1101/636514; this version posted May 11, 2020. The copyright holder for this preprint (which was not certified by peer review) is the author/funder, who has granted bioRxiv a license to display the preprint in perpetuity. It is made available under aCC-BY-NC-ND 4.0 International license.

de Vienne D, Leonardi A, Damerval C, Zivy M. 1999. Genetics of proteome variation for QTL characterization: application to drought-stress responses in maize. *J Exp Bot* **50**: 303–309.

Feltus FA. 2014. Systems genetics: a paradigm to improve discovery of candidate genes and mechanisms underlying complex traits. *Plant Sci* **223**: 45–48.

Feng S, Yue R, Tao S, Yang Y, Zhang L, Xu M, Wang H, Shen C. 2015. Genome-wide identification, expression analysis of auxin-responsive GH3 family genes in maize (Zea mays L.) under abiotic stresses. *J Integr Plant Biol* **57**: 783–795.

Ferry-Dumazet H, Houel G, Montalent P, Moreau L, Langella O, Negroni L, Vincent D, Lalanne C, de Daruvar A, Plomion C, et al. 2005. PROTICdb: A web-based application to store, track, query, and compare plant proteome data. *Proteomics* **5**: 2069–2081.

Forestan C, Aiese Cigliano R, Farinati S, Lunardon A, Sanseverino W, Varotto S. 2016. Stress-induced and epigenetic-mediated maize transcriptome regulation study by means of transcriptome reannotation and differential expression analysis. *Sci Rep* **6**: 30446.

Foss EJ, Radulovic D, Shaffer SA, Goodlett DR, Kruglyak L, Bedalov A. 2011. Genetic variation shapes protein networks mainly through non-transcriptional mechanisms. *PLoS Biol* **9**: e1001144.

Ganal MW, Durstewitz G, Polley A, Bérard A, Buckler ES, Charcosset A, Clarke JD, Graner E-M, Hansen M, Joets J, et al. 2011. A large maize (Zea mays L.) SNP genotyping array: Development and germplasm genotyping, and genetic mapping to compare with the B73 reference genome. *PLoS ONE* **6**: e28334.

Ghazalpour A, Bennett B, Petyuk VA, Orozco L, Hagopian R, Mungrue IN, Farber CR, Sinsheimer J, Kang HM, Furlotte N, et al. 2011. Comparative analysis of proteome and transcriptome variation in mouse. *PLoS Genet* **7**: e1001393.

Goldman AD, Samudrala R, Baross JA. 2010. The evolution and functional repertoire of translation proteins following the origin of life. *Biol Direct* **5**: 15.

Golldack D, Li C, Mohan H, Probst N. 2014. Tolerance to drought and salt stress in plants: Unraveling the signaling networks. *Front Plant Sci* **5**.

Harrison MT, Tardieu F, Dong Z, Messina CD, Hammer GL. 2014. Characterizing drought stress and trait influence on maize yield under current and future conditions. *Glob Change Biol* **20**: 867–878.

Jiang L-G, Li B, Liu S-X, Wang H-W, Li C-P, Song S-H, Beatty M, Zastrow-Hayes G, Yang X-H, Qin F, et al. 2019. Characterization of proteome variation during modern maize breeding. *Mol Cell Proteomics* **18**: 263–276.

Keshishian H, Burgess MW, Specht H, Wallace L, Clauser KR, Gillette MA, Carr SA. 2017. Quantitative, multiplexed workflow for deep analysis of human blood plasma and biomarker discovery by mass spectrometry. *Nat Protoc* **12**: 1683–1701.

Langella O, Valot B, Balliau T, Blein-Nicolas M, Bonhomme L, Zivy M. 2017. X!TandemPipeline: A tool to manage sequence redundancy for protein inference and phosphosite identification. *J Proteome Res* **16**: 494–503.

Langella O, Valot B, Jacob D, Balliau T, Flores R, Hoogland C, Joets J, Zivy M. 2013. Management and dissemination of MS proteomic data with PROTICdb: example of a quantitative comparison between methods of protein extraction. *Proteomics* **13**: 1457–1466.

Langella O, Zivy M, Joets J. 2007. The PROTICdb database for 2-DE proteomics. *Methods Mol Biol* **355**: 279–303.

Langfelder P, Horvath S. 2008. WGCNA: an R package for weighted correlation network analysis. *BMC Bioinformatics* **9**: 559.

Lippert C, Listgarten J, Liu Y, Kadie CM, Davidson RI, Heckerman D. 2011. FaST linear mixed models for genome-wide association studies. *Nat Methods* **8**: 833–835.

bioRxiv preprint doi: https://doi.org/10.1101/636514; this version posted May 11, 2020. The copyright holder for this preprint (which was not certified by peer review) is the author/funder, who has granted bioRxiv a license to display the preprint in perpetuity. It is made available under aCC-BY-NC-ND 4.0 International license.

Lobell DB, Roberts MJ, Schlenker W, Braun N, Little BB, Rejesus RM, Hammer GL. 2014. Greater sensitivity to drought accompanies maize yield increase in the U.S. midwest. *Science* **344**: 516–519.

Mähler N, Wang J, Terebieniec BK, Ingvarsson PK, Street NR, Hvidsten TR. 2017. Gene co-expression network connectivity is an important determinant of selective constraint. *PLoS Genet* **13**: e1006402.

Mangin B, Siberchicot A, Nicolas S, Doligez A, This P, Cierco-Ayrolles C. 2012. Novel measures of linkage disequilibrium that correct the bias due to population structure and relatedness. *Heredity* **108**: 285–291.

Mao H-D, Yu L-J, Li Z-J, Yan Y, Han R, Liu H, Ma M. 2016. Genome-wide analysis of the SPL family transcription factors and their responses to abiotic stresses in maize. *Plant Gene* **6**: 1–12.

Markowetz F, Boutros M. 2015. An introduction to systems genetics. In *Systems Genetics* (eds. F. Markowetz and M. Boutros), pp. 1–11, Cambridge University Press, doi:10.1017/CBO9781139012751.001

Meng Q, Chen X, Lobell DB, Cui Z, Zhang Y, Yang H, Zhang F. 2016. Growing sensitivity of maize to water scarcity under climate change. *Sci Rep* **6**: 19605.

Mizrachi E, Verbeke L, Christie N, Fierro AC, Mansfield SD, Davis MF, Gjersing E, Tuskan GA, Montagu MV, Peer YV de, et al. 2017. Network-based integration of systems genetics data reveals pathways associated with lignocellulosic biomass accumulation and processing. *Proc Natl Acad Sci* **114**: 1195–1200.

Moreno-Moral A, Petretto E. 2016. From integrative genomics to systems genetics in the rat to link genotypes to phenotypes. *Dis Model Mech* **9**: 1097–1110.

Munkvold JD, Laudencia-Chingcuanco D, Sorrells ME. 2013. Systems genetics of environmental response in the mature wheat embryo. *Genetics* **194**: 265–277.

Nadeau JH, Dudley AM. 2011. Systems genetics. *Science* **331**: 1015–1016.

Negro SS, Millet EJ, Madur D, Bauland C, Combes V, Welcker C, Tardieu F, Charcosset A, Nicolas SD. 2019. Genotyping-by-sequencing and SNP-arrays are complementary for detecting quantitative trait loci by tagging different haplotypes in association studies. *BMC Plant Biol* **19**: 318.

Nelson N, Junge W. 2015. Structure and energy transfer in photosystems of oxygenic photosynthesis. *Annu Rev Biochem* **84**: 659–683.

Neveu P, Tireau A, Hilgert N, Nègre V, Mineau-Cesari J, Brichet N, Chapuis R, Sanchez I, Pommier C, Charnomordic B, et al. 2019. Dealing with multi-source and multi-scale information in plant phenomics: the ontology-driven Phenotyping Hybrid Information System. *New Phytol* **221**: 588–601.

Orozco LD, Bennett BJ, Farber CR, Ghazalpour A, Pan C, Che N, Wen P, Qi HX, Mutukulu A, Siemers N, et al. 2012. Unraveling inflammatory responses using systems genetics and gene-environment interactions in macrophages. *Cell* **151**: 658–670.

Osakabe Y, Osakabe K, Shinozaki K, Tran L-SP. 2014. Response of plants to water stress. *Front Plant Sci* **5**.

Popadin KY, Gutierrez-Arcelus M, Lappalainen T, Buil A, Steinberg J, Nikolaev SI, Lukowski SW, Bazykin GA, Seplyarskiy VB, Ioannidis P, et al. 2014. Gene age predicts the strength of purifying selection acting on gene expression variation in humans. *Am J Hum Genet* **95**: 660–674.

Prado SA, Cabrera-Bosquet L, Grau A, Coupel-Ledru A, Millet EJ, Welcker C, Tardieu F. 2018. Phenomics allows identification of genomic regions affecting maize stomatal conductance with conditional effects of water deficit and evaporative demand. *Plant Cell Environ* **41**: 314–326.

Preston JC, Hileman LC. 2013. Functional Evolution in the Plant SQUAMOSA-PROMOTER BINDING PROTEIN-LIKE (SPL) Gene Family. *Front Plant Sci* **4**: 80.

R core team. 2013. R: A language and environment for statistical computing. R Foundation for Statistical Computing, Vienna, Austria.

bioRxiv preprint doi: https://doi.org/10.1101/636514; this version posted May 11, 2020. The copyright holder for this preprint (which was not certified by peer review) is the author/funder, who has granted bioRxiv a license to display the preprint in perpetuity. It is made available under aCC-BY-NC-ND 4.0 International license.

Rincent R, Moreau L, Monod H, Kuhn E, Melchinger AE, Malvar RA, Moreno-Gonzalez J, Nicolas S, Madur D, Combes V, et al. 2014. Recovering power in association mapping panels with variable levels of linkage disequilibrium. *Genetics* **197**: 375–387.

Schittenhelm S, Schroetter S. 2014. Comparison of drought tolerance of maize, sweet sorghum and sorghum-sudangrass hybrids. *J Agron Crop Sci* **200**: 46–53.

Seki M, Umezawa T, Urano K, Shinozaki K. 2007. Regulatory metabolic networks in drought stress responses. *Curr Opin Plant Biol* **10**: 296–302.

Shannon P, Markiel A, Ozier O, Baliga NS, Wang JT, Ramage D, Amin N, Schwikowski B, Ideker T. 2003. Cytoscape: a software environment for integrated models of biomolecular interaction networks. *Genome Res* **13**: 2498–2504.

Shiferaw B, Prasanna BM, Hellin J, Bänziger M. 2011. Crops that feed the world 6. Past successes and future challenges to the role played by maize in global food security. *Food Secur* **3**: 307.

Shinozaki K, Yamagushi-shinozaki K. 2007. Gene networks involved in drought stress response and tolerance. *J Exp Bot* **58**:221-227.

Tardieu F, Simonneau T, Muller B. 2018. The physiological basis of drought tolerance in crop plants: A scenario-dependent probabilistic approach. *Annu Rev Plant Biol* **69**: 733–759.

Thimm O, Bläsing O, Gibon Y, Nagel A, Meyer S, Krüger P, Selbig J, Müller LA, Rhee SY, Stitt M. 2004. Mapman: a user-driven tool to display genomics data sets onto diagrams of metabolic pathways and other biological processes. *Plant J* **37**: 914–939.

Tripathi P, Rabara RC, Rushton PJ. 2014. A systems biology perspective on the role of WRKY transcription factors in drought responses in plants. *Planta* **239**: 255–266.

Unterseer S, Bauer E, Haberer G, Seidel M, Knaak C, Ouzunova M, Meitinger T, Strom TM, Fries R, Pausch H, et al. 2014. A powerful tool for genome analysis in maize: development and evaluation of the high density 600 k SNP genotyping array. *BMC Genomics* **15**: 823.

Usadel B, Poree F, Nagel A, Lohse M, Czedik-Eysenberg A, Stitt M. 2009. A guide to using MapMan to visualize and compare omics data in plants: a case study in the crop species, maize. *Plant Cell Environ* **32**: 1211–1229.

Valliyodan B, Nguyen HT. 2006. Understanding regulatory networks and engineering for enhanced drought tolerance in plants. *Curr Opin Plant Biol* **9**: 189–195.

Valot B, Langella O, Nano E, Zivy M. 2011. MassChroQ : A versatile tool for mass spectrometry quantification. *Proteomics* **11**: 3572–3577.

van der Sijde MR, Ng A, Fu J. 2014. Systems genetics: From GWAS to disease pathways. *Biochim Biophys Acta* **1842**: 1903–1909.

Vogel C, Marcotte EM. 2012. Insights into the regulation of protein abundance from proteomic and transcriptomic analyses. *Nat Rev Genet* **13**: 227–232.

Wang X, Cai X, Xu C, Wang Q, Dai S. 2016. Drought-responsive mechanisms in plant leaves revealed by proteomics. *Int J Mol Sci* **17**: 1706.

Wasinger VC, Zeng M, Yau Y. 2013. Current Status and Advances in Quantitative Proteomic Mass Spectrometry. *Int J Proteomics* 2013:180605

Yu J, Pressoir G, Briggs WH, Vroh Bi I, Yamasaki M, Doebley JF, McMullen MD, Gaut BS, Nielsen DM, Holland JB, et al. 2006. A unified mixed-model method for association mapping that accounts for multiple levels of relatedness. *Nat Genet* **38**: 203–208.

bioRxiv preprint doi: https://doi.org/10.1101/636514; this version posted May 11, 2020. The copyright holder for this preprint (which was not certified by peer review) is the author/funder, who has granted bioRxiv a license to display the preprint in perpetuity. It is made available under aCC-BY-NC-ND 4.0 International license.

Zegada-Lizarazu W, Zatta A, Monti A. 2012. Water uptake efficiency and above- and belowground biomass development of sweet sorghum and maize under different water regimes. *Plant Soil* **351**: 47–60.

Zhang J, Yang J-R. 2015. Determinants of the rate of protein sequence evolution. *Nat Rev Genet* **16**: 409–420.

Zipper SC, Qiu J, Kucharik CJ. 2016. Drought effects on US maize and soybean production: spatiotemporal patterns and historical changes. *Environ Res Lett* **11**: 094021.

bioRxiv preprint doi: https://doi.org/10.1101/636514; this version posted May 11, 2020. The copyright holder for this preprint (which was not certified by peer review) is the author/funder, who has granted bioRxiv a license to display the preprint in perpetuity. It is made available under aCC-BY-NC-ND 4.0 International license.

FIGURE LEGENDS

Figure 1. Effect of mild water deficit on the proteome. (A) Heatmap representations of protein abundances estimated for the XIC-based protein set (left) and the SC-based protein set (right). Each line corresponds to a protein and each column to a genotype x watering condition combination. For each protein, abundance values were scaled and represented by a color code as indicated by the color-key bar. Hierarchical clustering of the genotype x watering condition combinations (top) and of the proteins (left) was built using the 1- Pearson correlation coefficient as the distance and the unweighted pair group method with arithmetic mean (UPGMA) as the aggregation method. (B) Functions of the induced and repressed proteins under water deficit. (C) Abundance profiles of the RAB17 dehydrin (GRMZM2G079440 quantified based on the number of spectra) and of a LEA protein (GRMZM2G352415 quantified based on peptide intensity) in the two watering conditions. Genotypes on the x axis were ordered according to the WD/WW abundance ratio. The lists of genotypes in this order are available in Supplemental Table S2.

Figure 2. Relationship between the mean number of pQTLs per KEGG category and the mean heritability per KEGG category.

Figure 3. Distribution of pQTLs across the genome. (A) In the well-watered condition. (B) In the water deficit condition. Each point indicates the number of proteins associated with a pQTL located within a given genomic region defined by the linkage disequilibrium interval around an SNP. Dashed horizontal lines indicate the threshold used to detect pQTL hotspots. Names and positions of the pQTL hotspots are indicated above each graph. Asterisks indicate the pQTL hotspots confidently detected as loci with potential pleiotropic effects (details given in Supplemental Table S4).

bioRxiv preprint doi: https://doi.org/10.1101/636514; this version posted May 11, 2020. The copyright holder for this preprint (which was not certified by peer review) is the author/funder, who has granted bioRxiv a license to display the preprint in perpetuity. It is made available under aCC-BY-NC-ND 4.0 International license.

Figure 4. Graphical representation of the co-expression networks resulting from the WGCNA analysis. Only proteins with an adjacency > 0.02 are shown. The two views were created by Cytoscape v3.5.1 using an unweighted, spring-embedded layout (cytoscape files are available in Supplementary File S1). The colors displayed on each network represent the different modules identified by WGCNA. Functional enrichments of modules are indicated with corresponding colors. Condition-specific modules are circled. Each module contains 35 to 471 proteins.

Figure 5. Genomic position of the co-localizing pQTLs, coQTLs and QTLs. The positions of the fifteen pQTL hotspots confidently identified as loci with potential pleiotropic effects are indicated, as well as the positions of the most promising candidate genes. Chromosomes are segmented into 10 Mb bins. Grey dots represent the centromeres and blue dots indicate the position of genomic regions showing evidences for pleiotropy at both the proteome and phenotype level. Blue lines indicate co-localizations with QTLs that are determined by a same SNP.

° WD-specific module, * co-localization found in the WW condition

Figure 6. Identification of genomic regions associated with trait variations at multiple scales. (A) Distribution of the distances between co-localizing QTLs and pQTLs. (B) Detailed view of the QTL, pQTL, coQTL detected in the region covered by the Hs52d hotspot on Chromosome 5. Dots represent the SNPs determining the position of the QTLs and horizontal bars represent the linkage disequilibrium-based window around each SNP. Black circles indicate the pQTLs that co-localize with QTLs or coQTLs with a high correlation between protein abundance and the phenotypic trait value or the module eigengene. The position of two transcription factors (an SBP gene, GRMZM2G111136, and a C2C2-CO-like transcription factor, GRMZM2G148772) representing promising candidate genes are indicated.

bioRxiv preprint doi: https://doi.org/10.1101/636514; this version posted May 11, 2020. The copyright holder for this preprint (which was not certified by peer review) is the author/funder, who has granted bioRxiv a license to display the preprint in perpetuity. It is made available under aCC-BY-NC-ND 4.0 International license.

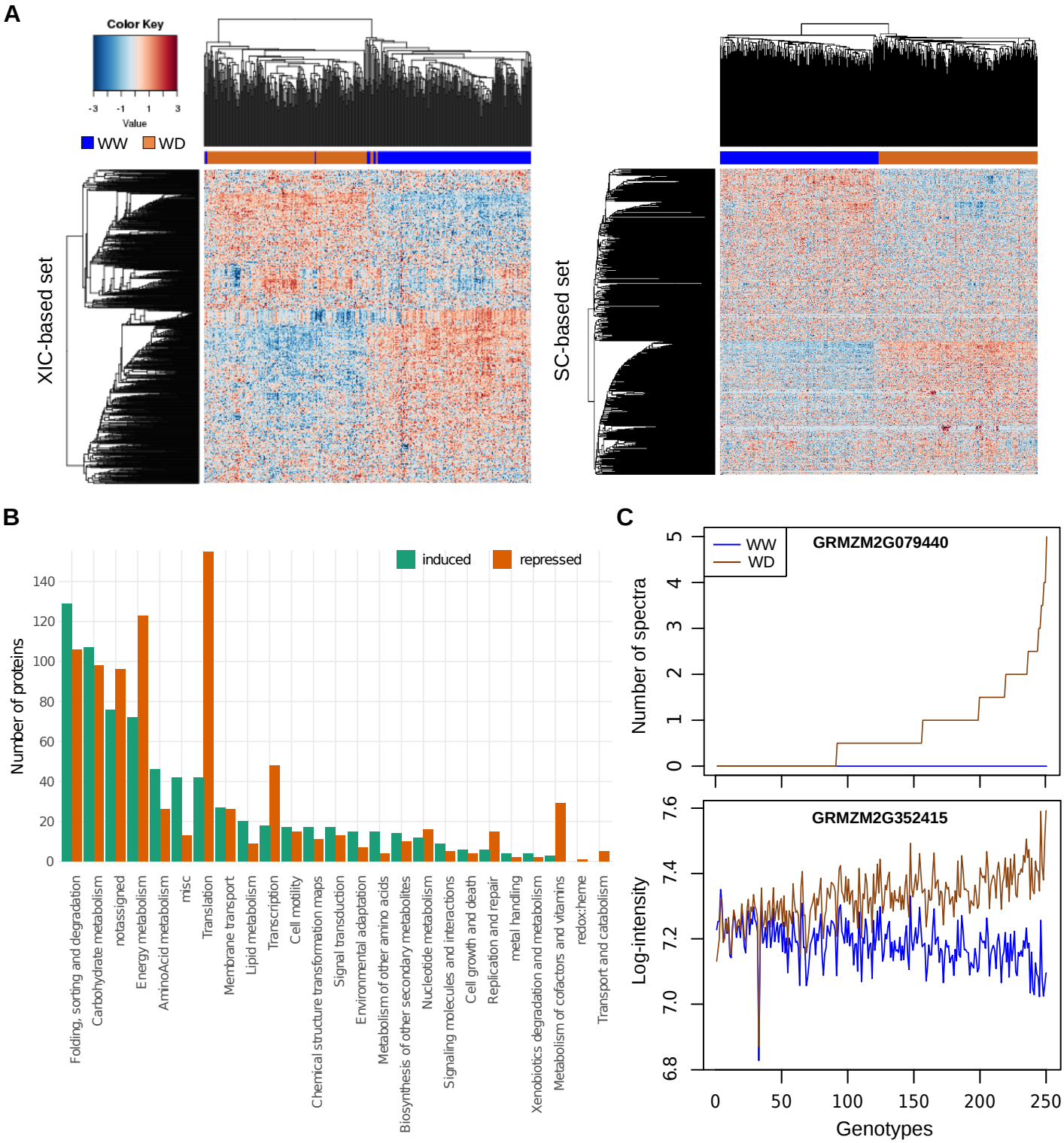

Figure 1. Effect of a mild water deficit on the proteome. (A) Heatmap representations of protein abundances estimated for the XIC-based protein set (left) and the SC-based protein set (right). Each line corresponds to a protein and each column to a genotype x watering condition combination. For each protein, abundance values were scaled and represented by a color code as indicated by the color-key bar. Hierarchical clustering of the genotype x watering condition combinations (top) and of the proteins (left) was built using the 1- Pearson correlation coefficient as the distance and the unweighted pair group method with arithmetic mean (UPGMA) as the aggregation method. (B) Functions of induced and repressed proteins under water deficit. (C) Abundance profiles of the RAB17 dehydrin (GRMZM2G079440 quantified based on the number of spectra) and of a LEA protein (GRMZM2G352415 quantified based on peptide intensity) in the two watering conditions. Genotypes on the x axis were ordered according to the WD/WW abundance ratio. The lists of genotypes in this order are available in Supplemental Table S2.

bioRxiv preprint doi: https://doi.org/10.1101/636514; this version posted May 11, 2020. The copyright holder for this preprint (which was not certified by peer review) is the author/funder, who has granted bioRxiv a license to display the preprint in perpetuity. It is made available under aCC-BY-NC-ND 4.0 International license.

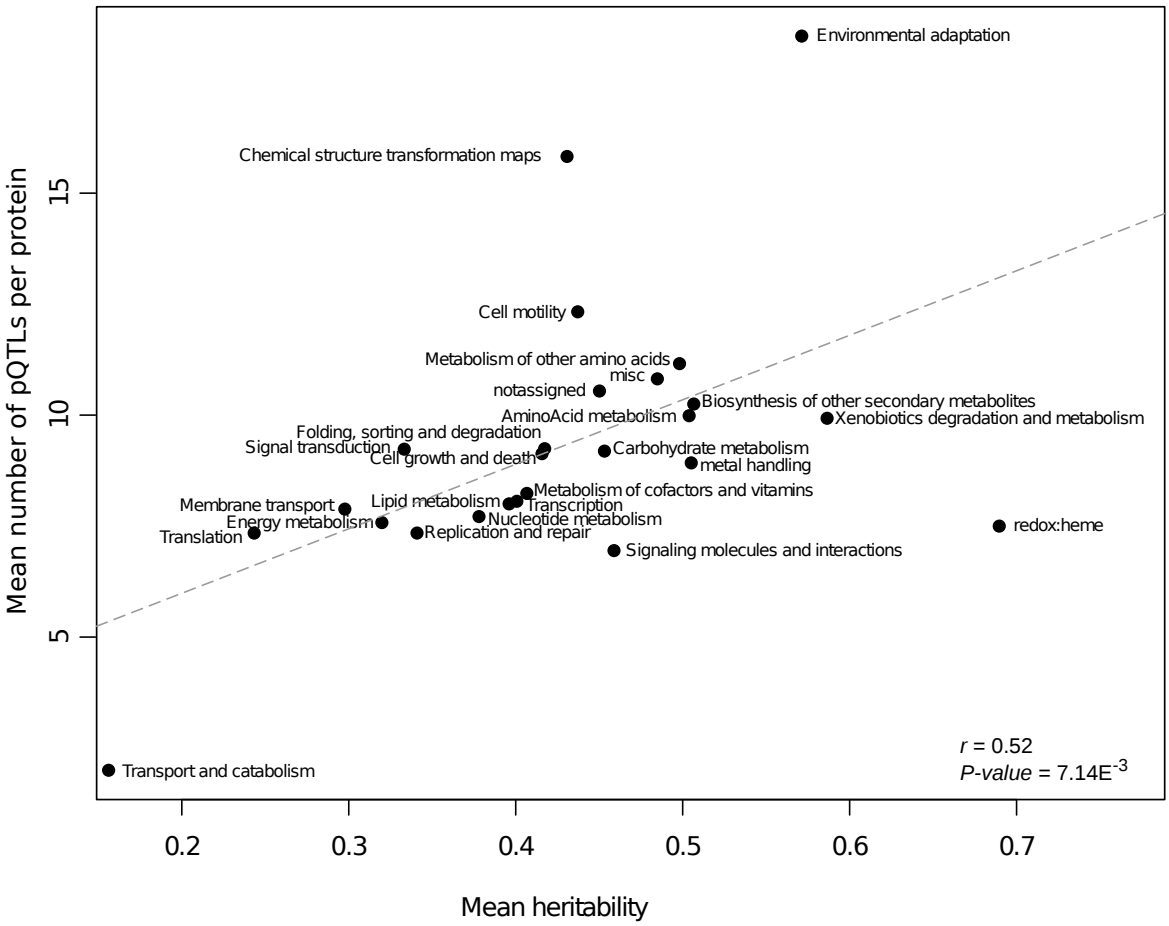

Figure 2. Relationship between the mean number of pQTLs per KEGG category and the mean heritability per KEGG category.

bioRxiv preprint doi: https://doi.org/10.1101/636514; this version posted May 11, 2020. The copyright holder for this preprint (which was not certified by peer review) is the author/funder, who has granted bioRxiv a license to display the preprint in perpetuity. It is made available under aCC-BY-NC-ND 4.0 International license.

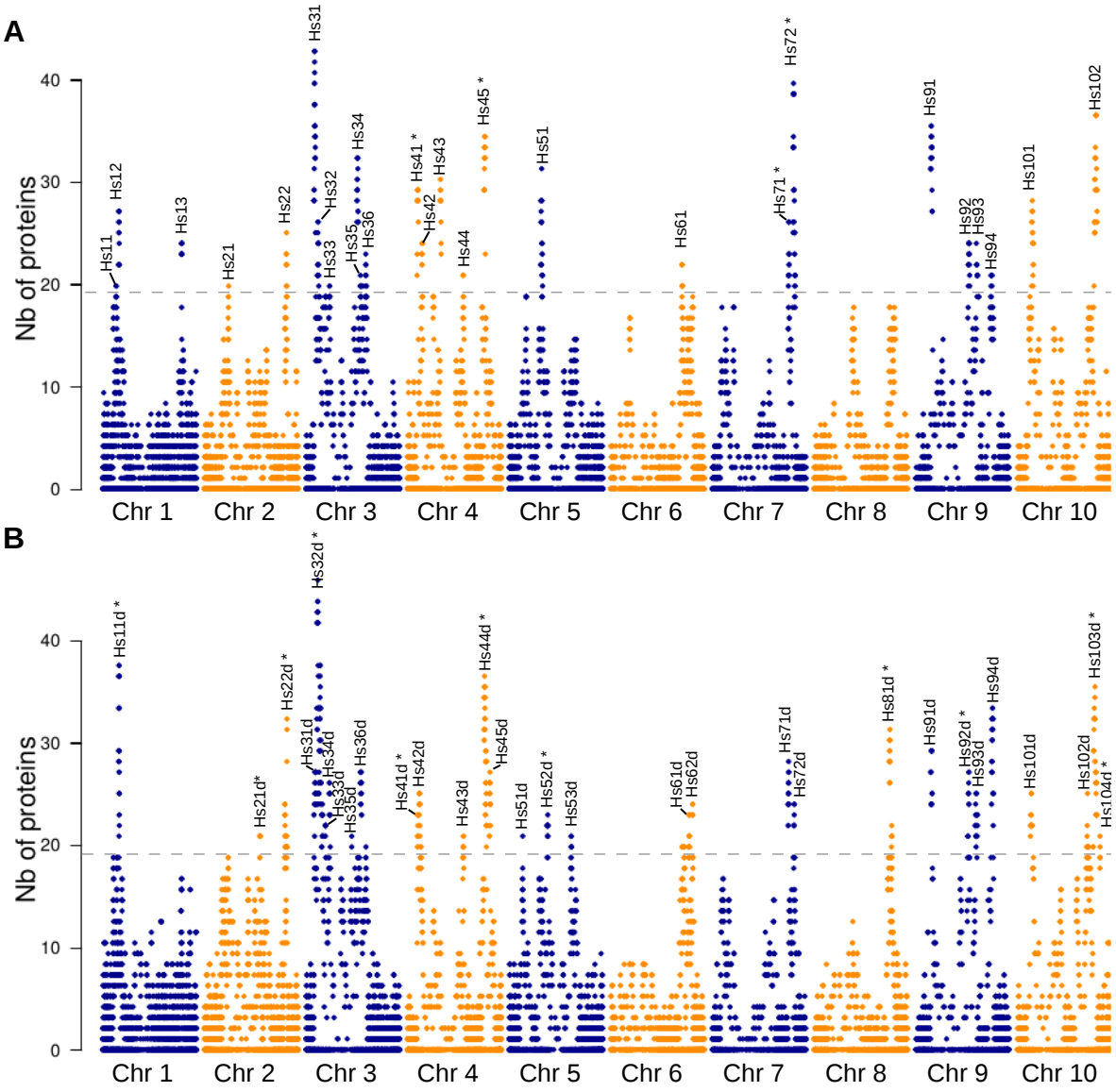

Figure 3. Distribution of pQTLs across the genome. (A) In the well-watered condition. (B) In the water deficit condition. Each point indicates the number of proteins controlled by a pQTL located within a given genomic region defined by the linkage disequilibrium interval around an SNP. Dashed horizontal lines indicate the threshold used to detect pQTL hotspots. Names and positions of the pQTL hotspots are indicated above each graph. Asterisks indicate the pQTL hotspots confidently detected as loci with potential pleiotropic effects (details given in Supplemental Table S4).

bioRxiv preprint doi: https://doi.org/10.1101/636514; this version posted May 11, 2020. The copyright holder for this preprint (which was not certified by peer review) is the author/funder, who has granted bioRxiv a license to display the preprint in perpetuity. It is made available under aCC-BY-NC-ND 4.0 International license.

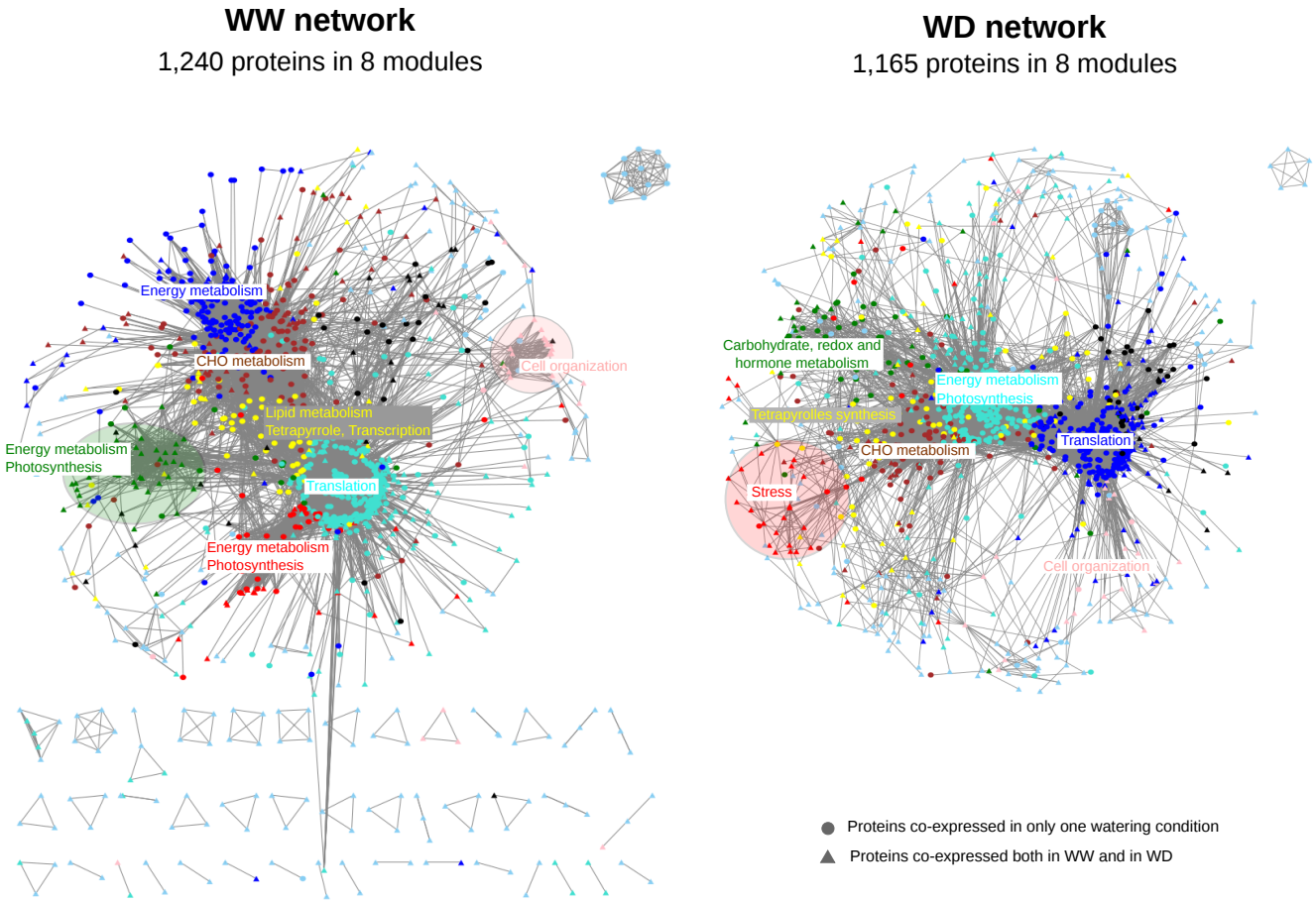

Figure 4. Graphical representation of the co-expression networks resulting from the WGCNA analysis. Only proteins with an adjacency > 0.02 are shown. The two views were created by Cytoscape v3.5.1 using an unweighted, spring-embedded layout (cytoscape files are available in Supplementary File S1). The colors displayed on each network represent the different modules identified by WGCNA. Functional enrichments of modules are indicated with corresponding colors. Condition-specific modules are circled. Each module contains 35 to 471 proteins.

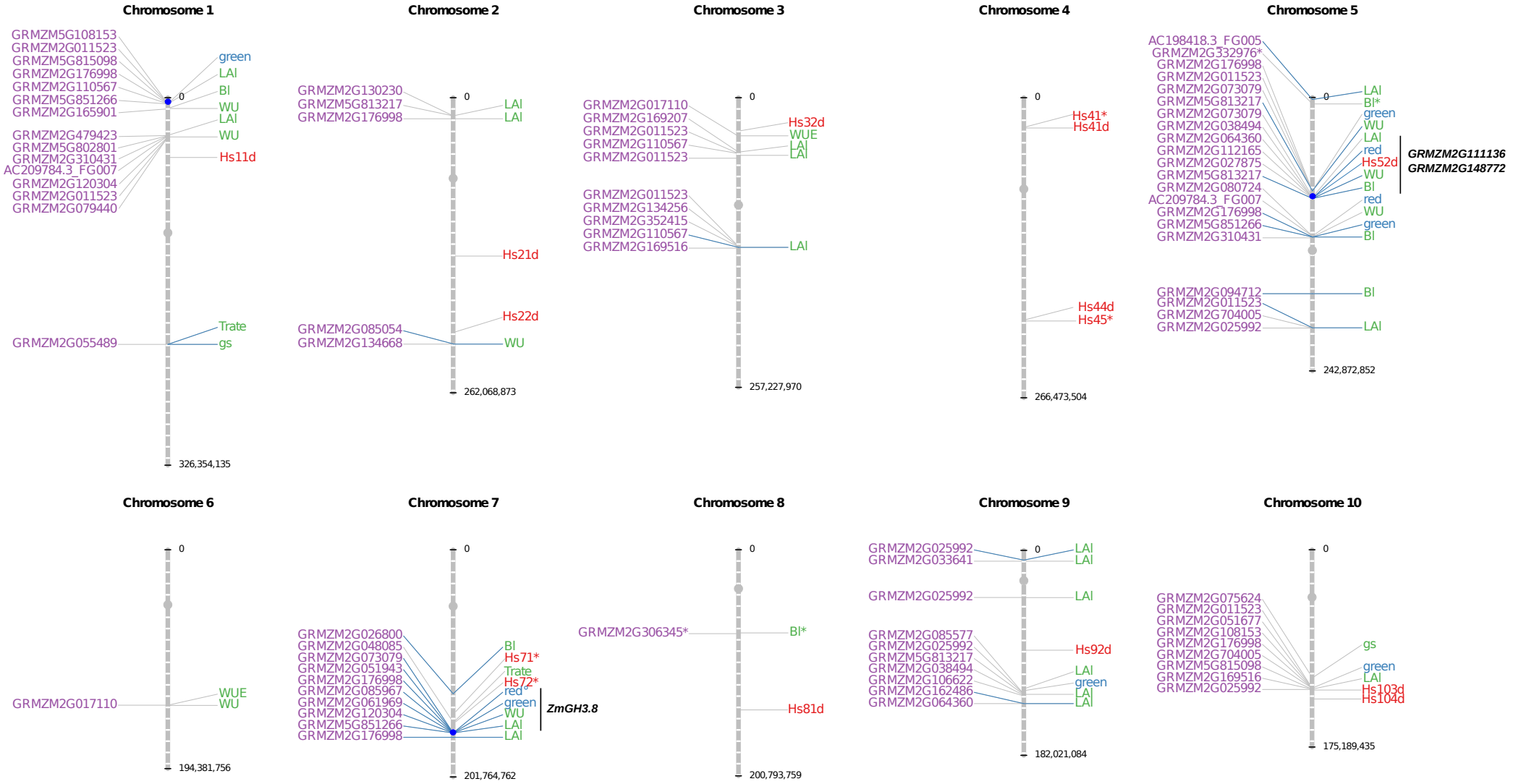

Figure 5. Genomic positions of the co-localizing pQTLs, coQTLs and QTLs. The positions of the fifteen pQTL hotspots confidently identified as loci with potential pleiotropic effects are indicated, as well as the position of the most promising candidate genes. Chromosomes are segmented into 10 Mb bins. Grey dots represent the centromeres and blue dots indicate the position of genomic regions showing evidences for pleiotropy at both the proteome and phenotype level. Blue lines indicate co-localizations with QTLs that are determined by a same SNP.

° WD-specific module, * co-localization found in the WW condition.

bioRxiv preprint doi: https://doi.org/10.1101/636514; this version posted May 11, 2020. The copyright holder for this preprint (which was not certified by peer review) is the author/funder, who has granted bioRxiv a license to display the preprint in perpetuity. It is made available under aCC-BY-NC-ND 4.0 International license.

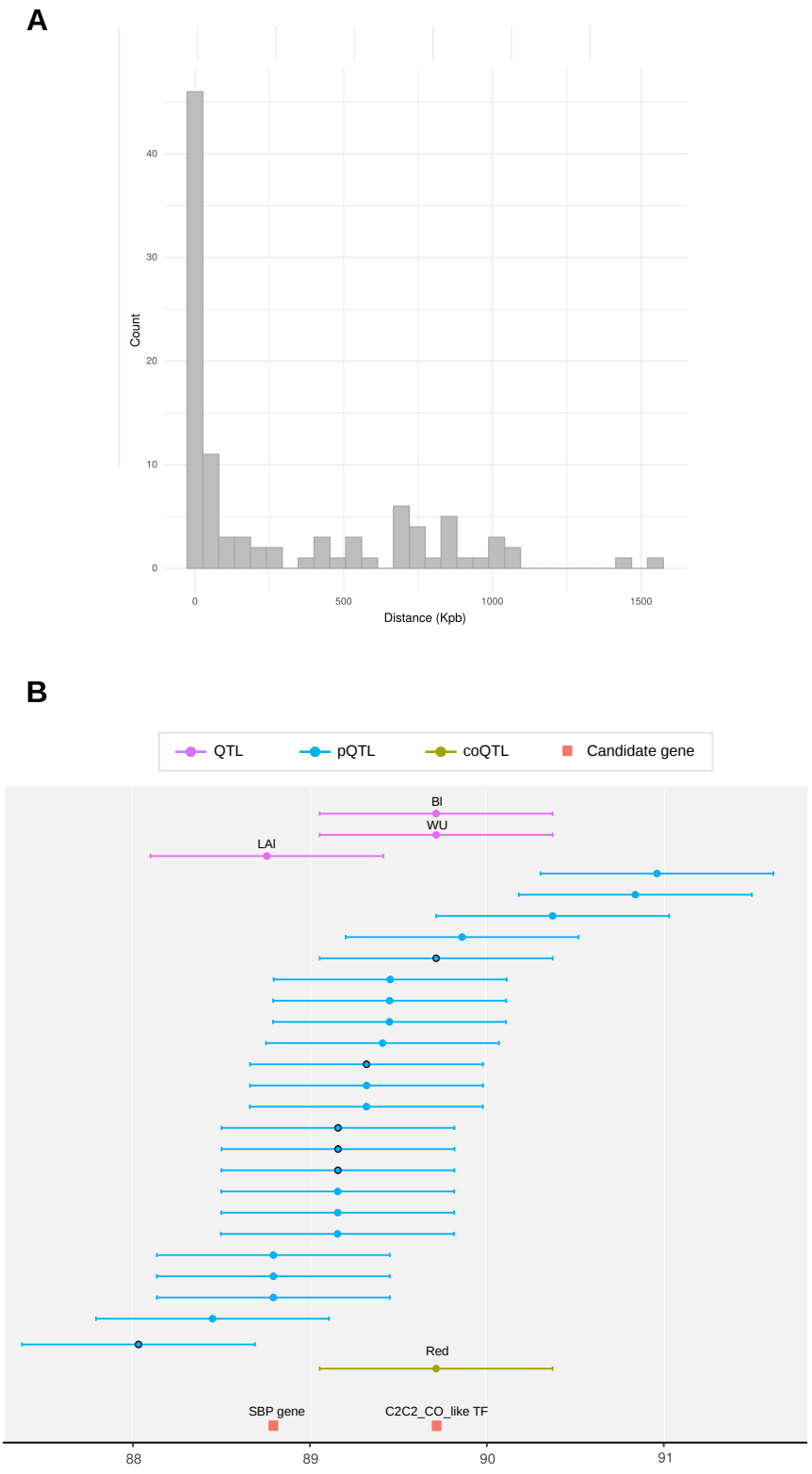

Figure 6. Identification of genomic regions involved in multi-scale genetic control.
(A) Distribution of the distances between co-localizing QTLs and pQTLs. (B) Detailed view of the QTL, pQTL, coQTL detected in the region covered by the Hs52d hotspot on chromosome 5. Dots represent the SNPs determining the position of the QTLs and horizontal bars represent the linkage disequilibrium-based window around each SNP. Black circles indicate the pQTLs that co-localize with QTLs or coQTLs with a high correlations between the protein abundance and the phenotypic trait value or the module eigengene. The position of two transcription factors (an SBP gene, GRMZM2G111136, and a C2C2-CO-like transcription factor, GRMZM2G148772) representing promising candidate genes are indicated.

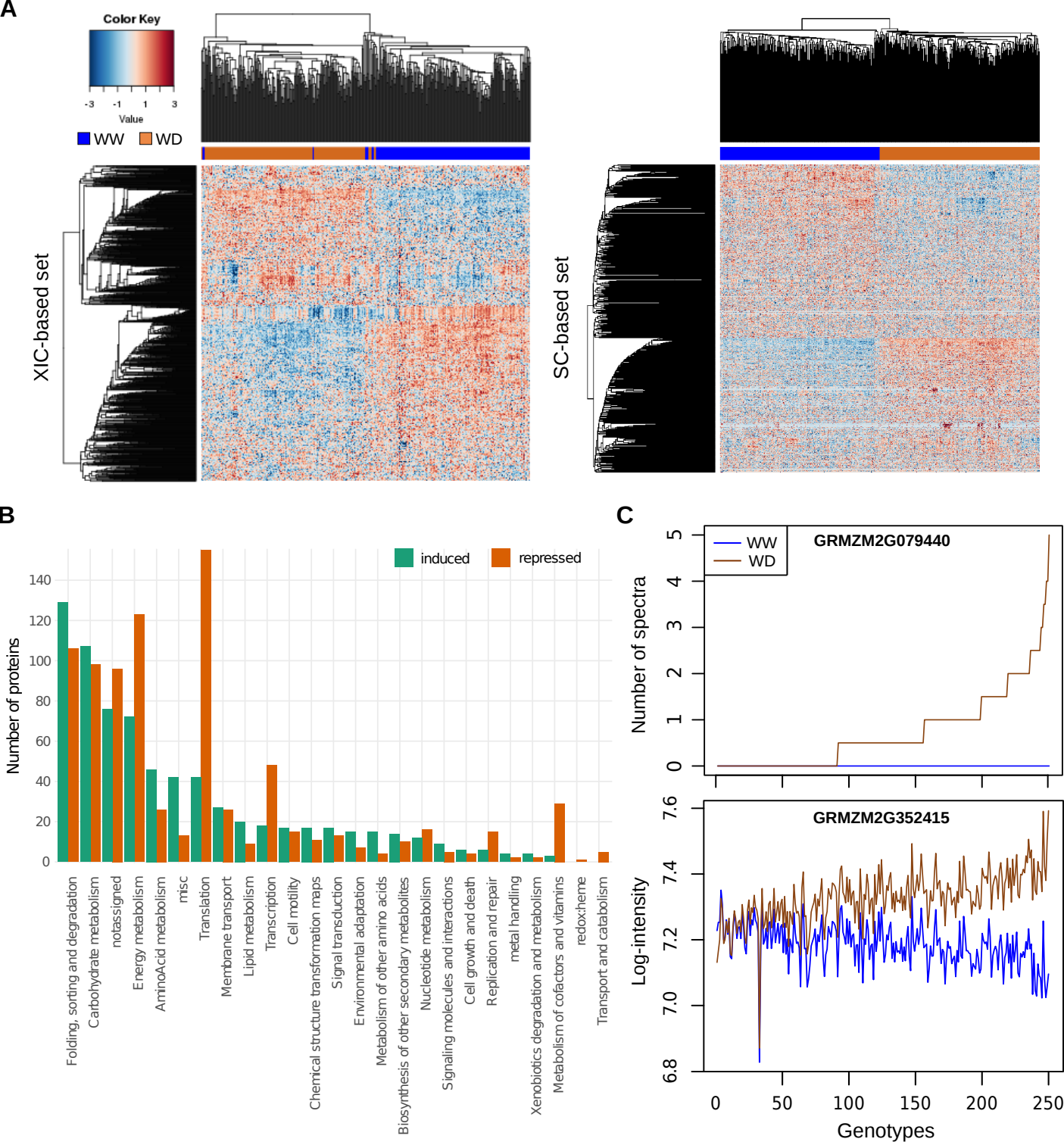
A
Color Key
-3 -1 1 3
Value
WW
WD
XIC-based set
SC-based set
B
induced
repressed
Number of proteins
0 20 40 60 80 100 120 140
Folding, sorting and degradation
Carbohydrate metabolism
notassigned
Energy metabolism
AminoAcid metabolism
misc
Translation
Membrane transport
Lipid metabolism
Transcription
Cell motility
Chemical structure transformation maps
Signal transduction
Environmental adaptation
Metabolism of other amino acids
Biosynthesis of other secondary metabolites
Nucleotide metabolism
Signaling molecules and interactions
Cell growth and death
Replication and repair
metal handling
Xenobiotics degradation and metabolism
Metabolism of cofactors and vitamins
redox:heme
Transport and catabolism
C
WW
WD
GRMZM2G079440
Number of spectra
0 1 2 3 4 5
GRMZM2G352415
Log-intensity
6.8 7.0 7.2 7.4 7.6
0 50 100 150 200 250
Genotypes

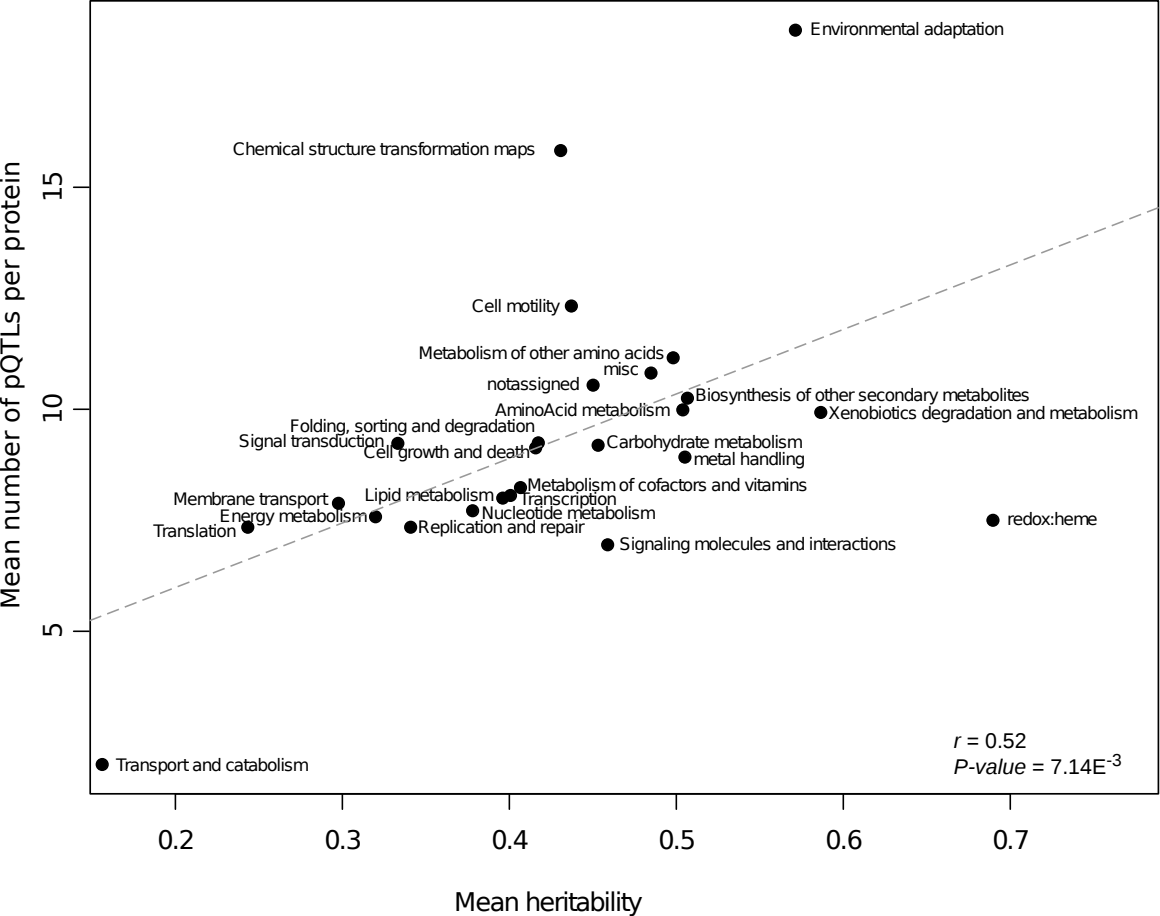
Environmental adaptation
Chemical structure transformation maps
Cell motility
Metabolism of other amino acids
misc
notassigned
Biosynthesis of other secondary metabolites
AminoAcid metabolism
Xenobiotics degradation and metabolism
Folding, sorting and degradation
Signal transduction
Cell growth and death
Carbohydrate metabolism
metal handling
Metabolism of cofactors and vitamins
Membrane transport
Lipid metabolism
Transcription
Energy metabolism
Nucleotide metabolism
redox:heme
Translation
Replication and repair
Signaling molecules and interactions
Transport and catabolism
r = 0.52
P-value = 7.14E-3
Mean number of pQTLs per protein
5
10
15
0.2
0.3
0.4
0.5
0.6
0.7
Mean heritability

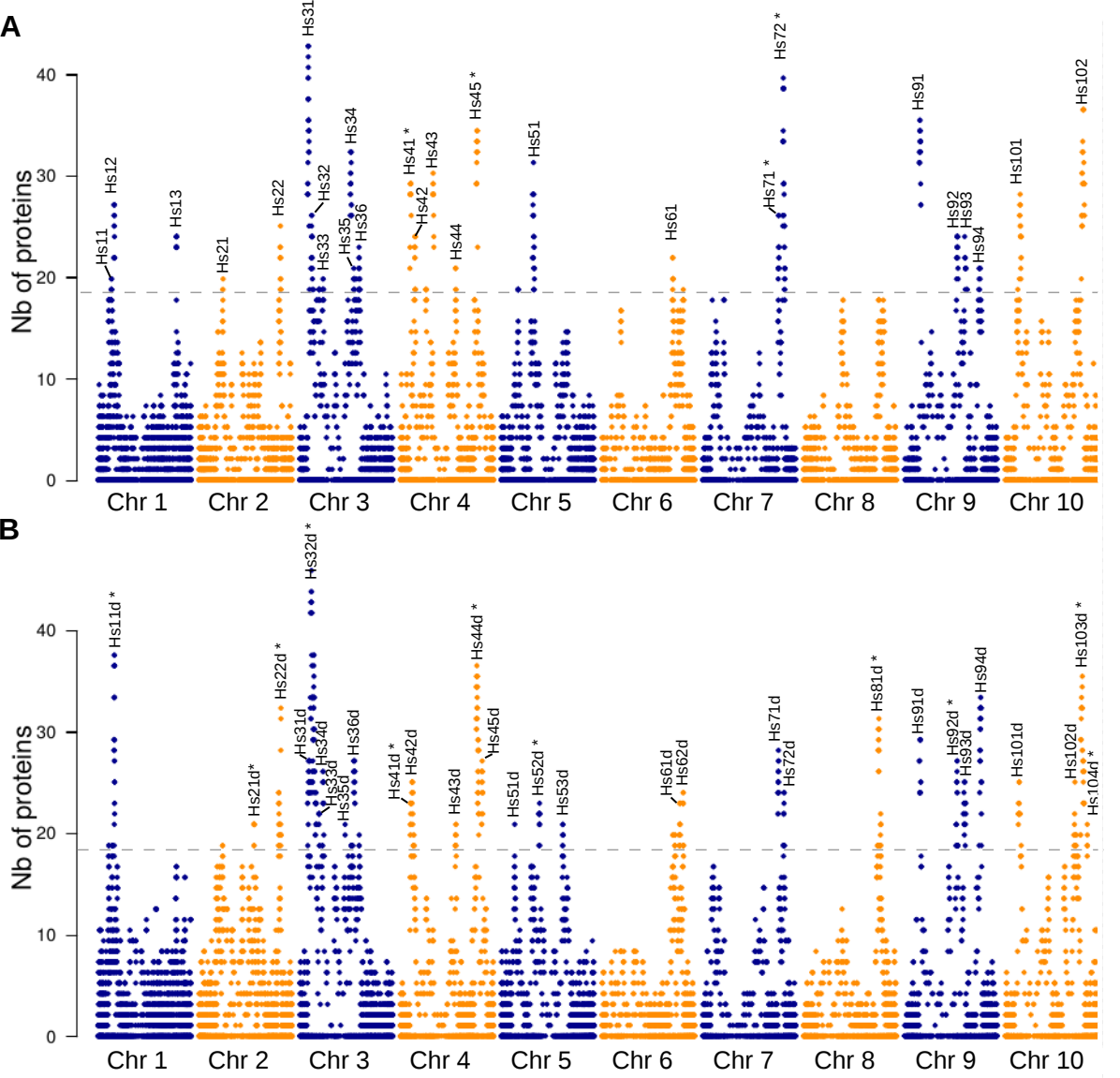
A
Nb of proteins
0
10
20
30
40
Hs11
Hs12
Hs13
Hs21
Hs22
Hs31
Hs32
Hs33
Hs34
Hs35
Hs36
Hs41 *
Hs42
Hs43
Hs44
Hs45 *
Hs51
Hs61
Hs71 *
Hs72 *
Hs91
Hs92
Hs93
Hs94
Hs101
Hs102
Chr 1
Chr 2
Chr 3
Chr 4
Chr 5
Chr 6
Chr 7
Chr 8
Chr 9
Chr 10
B
Nb of proteins
0
10
20
30
40
Hs11d *
Hs21d*
Hs22d *
Hs31d
Hs32d *
Hs33d
Hs34d
Hs35d
Hs36d
Hs41d *
Hs42d
Hs43d
Hs44d *
Hs45d
Hs51d
Hs52d *
Hs53d
Hs61d
Hs62d
Hs71d
Hs72d
Hs81d *
Hs91d
Hs92d *
Hs93d
Hs94d
Hs101d
Hs102d
Hs103d *
Hs104d *
Chr 1
Chr 2
Chr 3
Chr 4
Chr 5
Chr 6
Chr 7
Chr 8
Chr 9
Chr 10

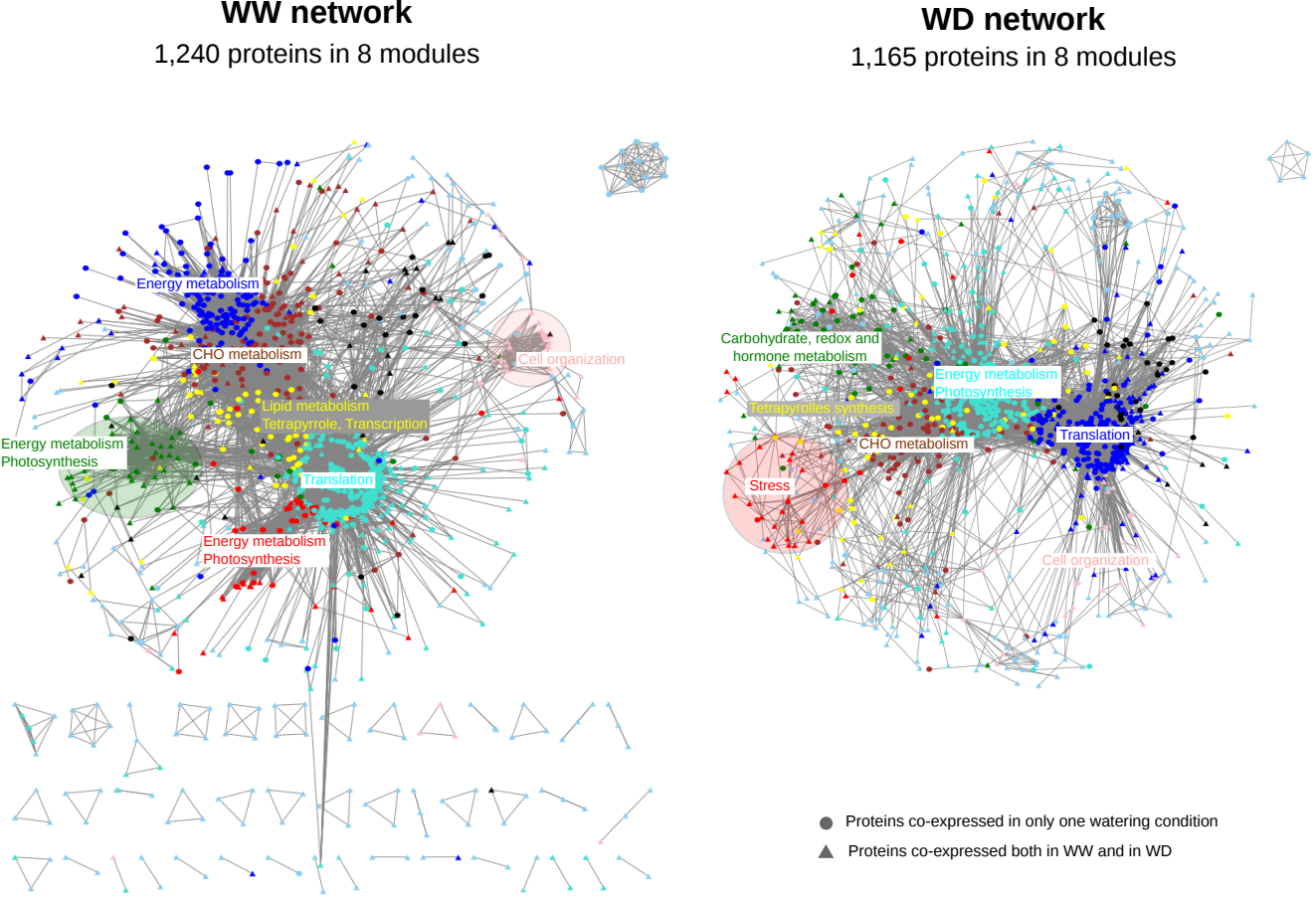
WW network
1,240 proteins in 8 modules
Energy metabolism
CHO metabolism
Cell organization
Lipid metabolism
Tetrapyrrole, Transcription
Energy metabolism
Photosynthesis
Translation
Energy metabolism
Photosynthesis
WD network
1,165 proteins in 8 modules
Carbohydrate, redox and
hormone metabolism
Energy metabolism
Photosynthesis
Tetrapyrolles synthesis
Translation
CHO metabolism
Stress
Cell organization
Proteins co-expressed in only one watering condition
Proteins co-expressed both in WW and in WD

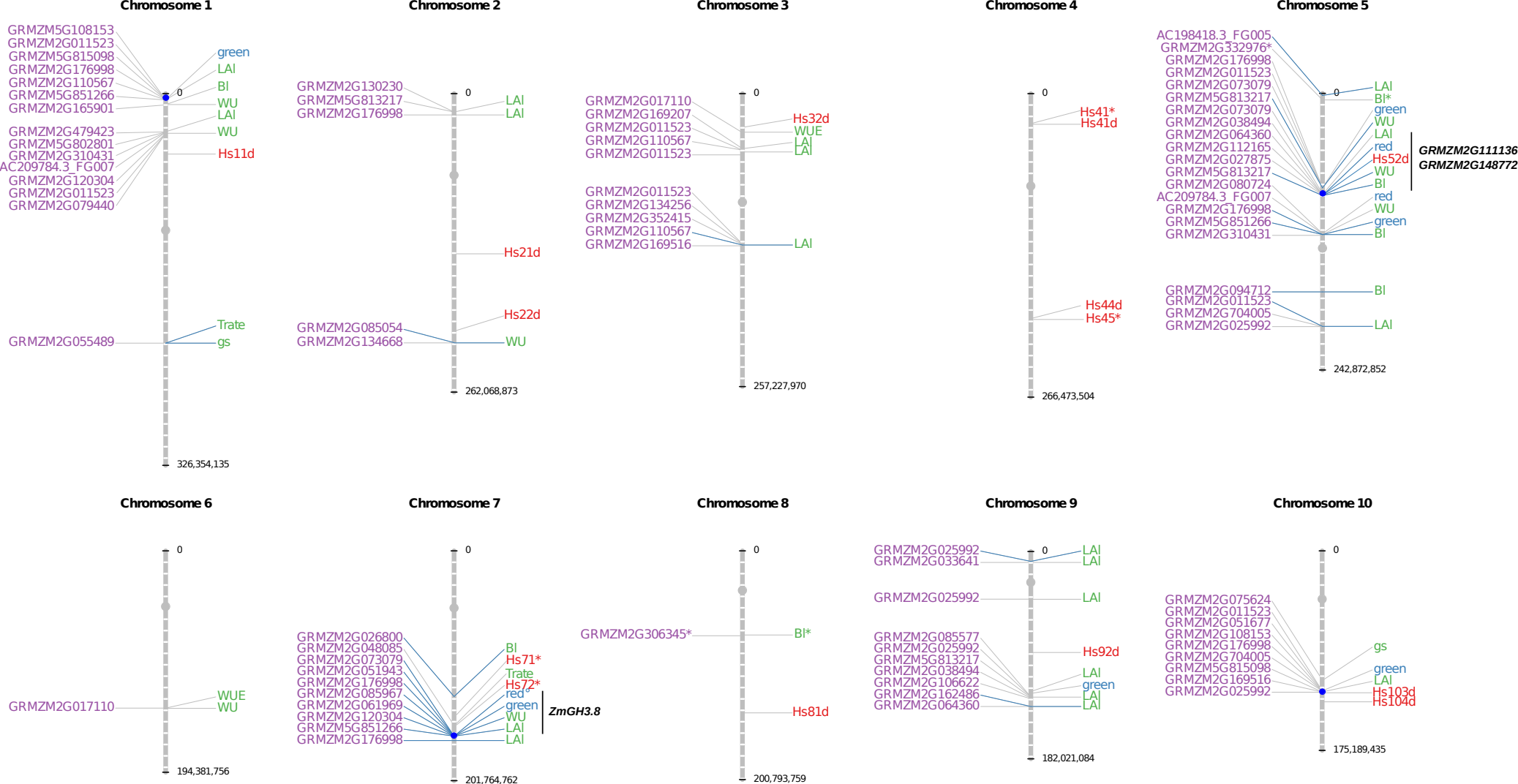
Chromosome 1
GRMZM5G108153
GRMZM2G011523
GRMZM5G815098
GRMZM2G176998
GRMZM2G110567
GRMZM5G851266
GRMZM2G165901
GRMZM2G479423
GRMZM5G802801
GRMZM2G310431
AC209784.3_FG007
GRMZM2G120304
GRMZM2G011523
GRMZM2G079440
GRMZM2G055489
green
LAI
BI
WU
LAI
WU
Hs11d
Trate
gs
0
326,354,135
Chromosome 2
GRMZM2G130230
GRMZM5G813217
GRMZM2G176998
GRMZM2G085054
GRMZM2G134668
LAI
LAI
Hs21d
Hs22d
WU
0
262,068,873
Chromosome 3
GRMZM2G017110
GRMZM2G169207
GRMZM2G011523
GRMZM2G110567
GRMZM2G011523
GRMZM2G011523
GRMZM2G134256
GRMZM2G352415
GRMZM2G110567
GRMZM2G169516
Hs32d
WUE
LAI
LAI
LAI
0
257,227,970
Chromosome 4
Hs41*
Hs41d
Hs44d
Hs45*
0
266,473,504
Chromosome 5
AC198418.3_FG005
GRMZM2G332976*
GRMZM2G176998
GRMZM2G011523
GRMZM2G073079
GRMZM5G813217
GRMZM2G073079
GRMZM2G038494
GRMZM2G064360
GRMZM2G112165
GRMZM2G027875
GRMZM5G813217
GRMZM2G080724
AC209784.3_FG007
GRMZM2G176998
GRMZM5G851266
GRMZM2G310431
GRMZM2G094712
GRMZM2G011523
GRMZM2G704005
GRMZM2G025992
LAI
BI*
green
WU
LAI
red
Hs52d
WU
BI
red
WU
green
BI
BI
LAI
GRMZM2G111136
GRMZM2G148772
0
242,872,852
Chromosome 6
GRMZM2G017110
WUE
WU
0
194,381,756
Chromosome 7
GRMZM2G026800
GRMZM2G048085
GRMZM2G073079
GRMZM2G051943
GRMZM2G176998
GRMZM2G085967
GRMZM2G061969
GRMZM2G120304
GRMZM5G851266
GRMZM2G176998
BI
Hs71*
Trate
Hs72*
red*
green
WU
LAI
LAI
ZmGH3.8
0
201,764,762
Chromosome 8
GRMZM2G306345*
BI*
Hs81d
0
200,793,759
Chromosome 9
GRMZM2G025992
GRMZM2G033641
GRMZM2G025992
GRMZM2G085577
GRMZM2G025992
GRMZM5G813217
GRMZM2G038494
GRMZM2G106622
GRMZM2G162486
GRMZM2G064360
LAI
LAI
LAI
Hs92d
LAI
green
LAI
LAI
0
182,021,084
Chromosome 10
GRMZM2G075624
GRMZM2G011523
GRMZM2G051677
GRMZM2G108153
GRMZM2G176998
GRMZM2G704005
GRMZM5G815098
GRMZM2G169516
GRMZM2G025992
gs
green
LAI
Hs103d
Hs104d
0
175,189,435

A

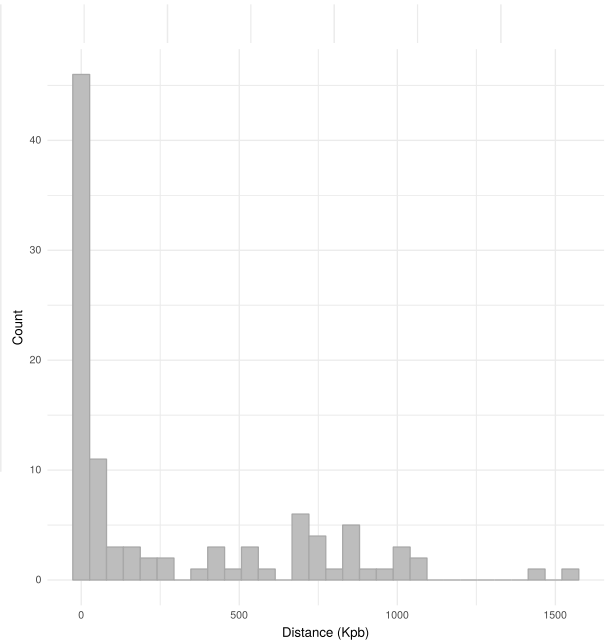
Count
40
30
20
10
0
0
500
1000
1500
Distance (Kpb)

B

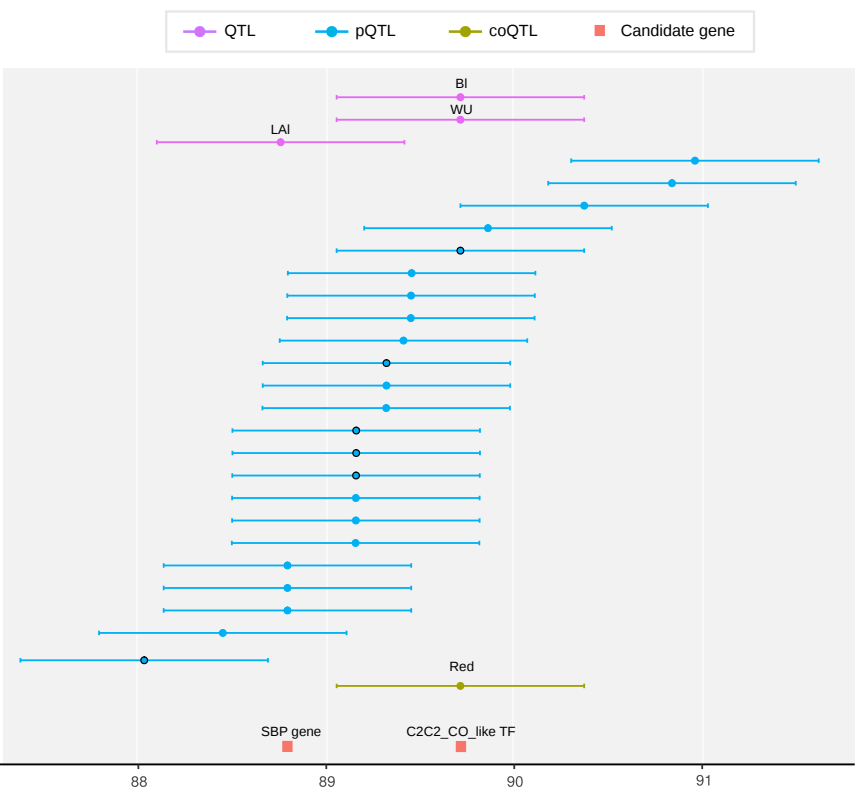
QTL
pQTL
coQTL
Candidate gene
BI
WU
LAI
Red
SBP gene
C2C2_CO_like TF
88
89
90
91